Title
The tropical forest and fire emissions experiment: Emission, chemistry, and transport of biogenic volatile organic compounds in the lower atmosphere over Amazonia

Journal
Journal of Geophysical Research, 112(D18)

ISSN
0148-0227

Authors
Karl, Thomas
Guenther, Alex
Yokelson, Robert J
et al.

Publication Date
2007

DOI
10.1029/2007jd008539

The tropical forest and fire emissions experiment: Emission, chemistry, and transport of biogenic volatile organic compounds in the lower atmosphere over Amazonia

Thomas Karl,[1] Alex Guenther,[1] Robert J. Yokelson,[2] Jim Greenberg,[1] Mark Potosnak,[3] Donald R. Blake,[4] and Paulo Artaxo[5]

Received 13 February 2007; revised 30 April 2007; accepted 14 May 2007; published 19 September 2007.

[1] Airborne and ground-based mixing ratio and flux measurements using eddy covariance (EC) and for the first time the mixed layer gradient (MLG) and mixed layer variance (MLV) techniques are used to assess the impact of isoprene and monoterpene emissions on atmospheric chemistry in the Amazon basin. Average noon isoprene (7.8 ± 2.3 mg/m^2/h) and monoterpene fluxes (1.2 ± 0.5 mg/m^2/h) compared well between ground and airborne measurements and are higher than fluxes estimated in this region during other seasons. The biogenic emission model, Model of Emissions of Gases and Aerosols from Nature (MEGAN), estimates fluxes that are within the model and measurement uncertainty and can describe the large observed variations associated with land-use change in the region north-west of Manaus. Isoprene and monoterpenes accounted for ~75% of the total OH reactivity in this region and are important volatile organic compounds (VOCs) for modeling atmospheric chemistry in Amazonia. The presence of fair weather clouds (*cumulus humilis*) had an important impact on the vertical distribution and chemistry of VOCs through the planetary boundary layer (PBL), the cloud layer, and the free troposphere (FT). Entrainment velocities between 10:00 and 11:30 local time (LT) are calculated to be on the order of 8–10 cm/s. The ratio of methyl-vinyl-ketone (MVK) and methacrolein (MAC) (unique oxidation products of isoprene chemistry) with respect to isoprene showed a pronounced increase in the cloud layer due to entrainment and an increased oxidative capacity in broken cloud decks. A decrease of the ratio in the lower free troposphere suggests cloud venting through activated clouds. OH modeled in the planetary boundary layer using a photochemical box model is much lower than OH calculated from a mixed layer budget approach. An ambient reactive sesquiterpene mixing ratio of 1% of isoprene would be sufficient to explain most of this discrepancy. Increased OH production due to increased photolysis in the cloud layer balances the low OH values modeled for the planetary boundary layer. The intensity of segregation (I_s) of isoprene and OH, defined as a relative reduction of the reaction rate constant due to incomplete mixing, is found to be significant: up to $39 \pm 7\%$ in the ~800-m-deep cloud layer. The effective reaction rate between isoprene and OH can therefore vary significantly in certain parts of the lower atmosphere.

Citation: Karl, T., A. Guenther, R. J. Yokelson, J. Greenberg, M. Potosnak, D. R. Blake, and P. Artaxo (2007), The tropical forest and fire emissions experiment: Emission, chemistry, and transport of biogenic volatile organic compounds in the lower atmosphere over Amazonia, *J. Geophys. Res.*, *112*, D18302, doi:10.1029/2007JD008539.

1. Introduction

[2] Biogenic volatile organic compound (VOC) emissions play a crucial role in fueling tropospheric air chemistry [*Fuentes et al.*, 2000; *Trainer et al.*, 1987]. According to bottom-up estimates, these emissions account for more than 80% of the total global VOC input [*Olivier and Berdowski*, 2001]. The tropics are of particular importance because more than 70% of the global total biogenic VOC flux occurs there. Yet, only a few direct measurements [*Crutzen et al.*, 2000; *Greenberg et al.*, 1999a, 1999b, 2004; *Karl et al.*, 2004; *Kesselmeier et al.*, 2000, 2002; *Kuhn et al.*,

[1]National Center for Atmospheric Research, Boulder, Colorado, USA.
[2]Department of Chemistry, University of Montana, Missoula, Montana, USA.
[3]Desert Research Institute, Reno, Nevada, USA.
[4]Department of Chemistry, University of California, Irvine, California, USA.
[5]University of Sao Paulo, Sao Paulo, Brazil.

0148-0227/07/2007JD008539

2002; *Rasmussen and Khalil*, 1988; *Rinne et al.*, 2002; *Warneke et al.*, 2001; *Zimmerman et al.*, 1988] are available from tropical regions to constrain global bottom-up emission models and estimates. Species distributions [*Harley et al.*, 2004], long-term variations [*Petron et al.*, 2001] as well as land-use change [*Guenther et al.*, 2006] are among the most uncertain aspects of scaling biogenic emissions up to the regional and global system.

[3] VOCs emitted by vegetation are transported upward in the planetary boundary layer (PBL) by turbulent diffusion and convection during daytime. At the same time, these compounds, i.e., isoprene and monoterpenes, react with oxidants (OH, O_3, and NO_3) on timescales similar to turnaround times in the convective PBL. Isoprene is a key compound constraining the oxidative capacity of the remote tropical atmosphere. The short lifetimes result in steep concentration gradients at the entrainment zone between the top of the PBL and the free troposphere (FT). Entrainment due to PBL growth in tropical regions typically occurs parallel with the development of broken cloud decks (*cumulus humilis*), some of which can grow into deep convective storms in the afternoon. The exchange of reactive VOCs between FT and PBL air occurs through consequent entrainment, cloud venting, and subsidence [e.g., *Ching and Alkezweeny*, 1986; *Angevine*, 2005]. Clouds also modify the radiation regime, which has a direct impact on the oxidative capacity of the atmosphere, and leads to the segregation of chemicals. While segregation effects, defined as relative reduction of reaction rate constants due to incomplete mixing, of VOCs are generally considered small [*Krol et al.*, 2000; *Verver et al.*, 2000], some modeling studies [*Vinuesa and de Arellano*, 2005] suggest that segregation of radical chemistry in the convective boundary layer could become significant under certain conditions.

[4] Not too surprisingly, these complex exchange processes lead to considerable uncertainty in modeling tropospheric chemistry in pristine tropical regions [*Crutzen et al.*, 2000; *Ganzeveld et al.*, 2002; *Kuhlmann et al.*, 2003]. For example, most global three-dimensional chemistry-transport models (3D-CT models) [*Bey et al.*, 2001] assume smaller (i.e., 20%) primary biogenic emissions than the (G95) bottom-up estimates [*Guenther et al.*, 1995]. *Kuhlmann et al.* [2003] reduced the G95 isoprene emission rates by 50% for tropical regions in order to adjust isoprene concentrations in the model PBL to values measured during various field observations. Similarly, the Intergovernmental Panel on Climate Change (IPCC) Working Group on Atmospheric Chemistry and Greenhouse Gases [*Ehhalt and Prather*, 2001] recommended using a global isoprene emission rate that is 56% lower than the G95 estimates. This emission reduction was used to produce chemistry and transport model simulations of CO and isoprene concentrations that were similar to observations. Satellite-derived isoprene emissions [*Palmer et al.*, 2003] based on formaldehyde (HCHO) columns are higher than isoprene fluxes calculated from G95 over North America and lower over tropical regions. Due to strong HCHO production from fires, the presence of clouds, and uncertainties associated with Global Ozone Monitoring Experiment (GOME) HCHO retrievals, satellite-based emission estimates of isoprene, however, are very uncertain in tropical regions (i.e., >90%) [*Shim et al.*, 2005]. Recently, biogenic VOC emission projections from the Model of Emissions of Gases and Aerosols from Nature (MEGAN) have become available [*Guenther et al.*, 2006] (G06). These projections are based on the latest emission measurement inputs and they suggest that the global emission strength, at least for isoprene, is about the same as G95 (i.e., 500–750 Tg/y). However, regional differences depending on land cover databases can be large.

[5] In order to shed light on some of the uncertainties associated with the emission of VOCs and their impact on atmospheric chemistry in tropical regions, we conducted the Tropical Forest and Fire Emissions Experiment (TROFFEE) [*Yokelson et al.*, 2007] during the 2004 dry season (August to September). The study included airborne and ground-based measurements above pristine tropical rain forest minimally impacted by biomass burning. Here we describe airborne vertical and horizontal concentration profiles complemented by ground-based eddy covariance (EC) measurements in the Amazon basin upwind of Manaus. We assess uncertainties associated with emissions, chemistry, and vertical transport of reactive biogenic VOCs and investigate the impact of land-use change on isoprene emissions.

2. Experimental Details

2.1. Measurement Location and Setup

[6] Measurements on an instrumented flux tower were conducted between 14 and 29 September 2004. The tower (Z14: −2.612, −60.21) is situated 60 km NNW of Manaus in Central Amazonia. The average canopy height around the tower (55 m) is 30 m with a leaf area index about 5–6. For flux measurements, a 40-m paraformaldehyde (PFA)-Teflon line (inner diameter (I.D.) 1/4 in.) pumped by a diaphragm pump (Pfeiffer, MD4) was used to draw air down into the measurement container situated at the tower. A flow of 15 sccm of this airstream was introduced into the proton transfer reaction mass spectrometry (PTR-MS) instrument. The pressure in the 40-m PFA-Teflon line (I.D. 0.635 mm) was reduced to 500 mbar in order to avoid condensation, minimize memory effects and assure a fast response time. The overall response time caused a delay time of less than 6 s, measured by spiking an isoprene pulse at the top of the tower. Air samples (typically 2 l) were collected in two-stage solid absorbent tubes (carbotrap/carbosieve, Supelco Inc., Bellefonte, PA) 10 m above the canopy.

[7] The airborne part of the TROFFEE campaign consisted of 44.5 flight hours between 27 August and 8 September 2004 on an Embraer 110B belonging to the Brazilian National Institute for Space Research (Instituto Nacional de Pesquisas Espaciais (INPE)). The aircraft was primarily based in Alta Floresta, Mato Grosso in the southern Amazon (−9.917, −56.017), and also near Manaus, Amazonas. On the aircraft, air was pulled through a 4-m backward facing Teflon line (I.D. 0.635 mm). The pressure inside the line was reduced to ∼70% of ambient pressure to avoid water condensation. The overall delay time was ∼1 s, measured by introducing an isoprene and acetone pulse at the inlet. Here we report observations obtained during the last portion of the deployment, when the research aircraft was based out of Manaus, Amazonas. Figure 1 shows flight tracks flown on 6 and 7 September 2004.

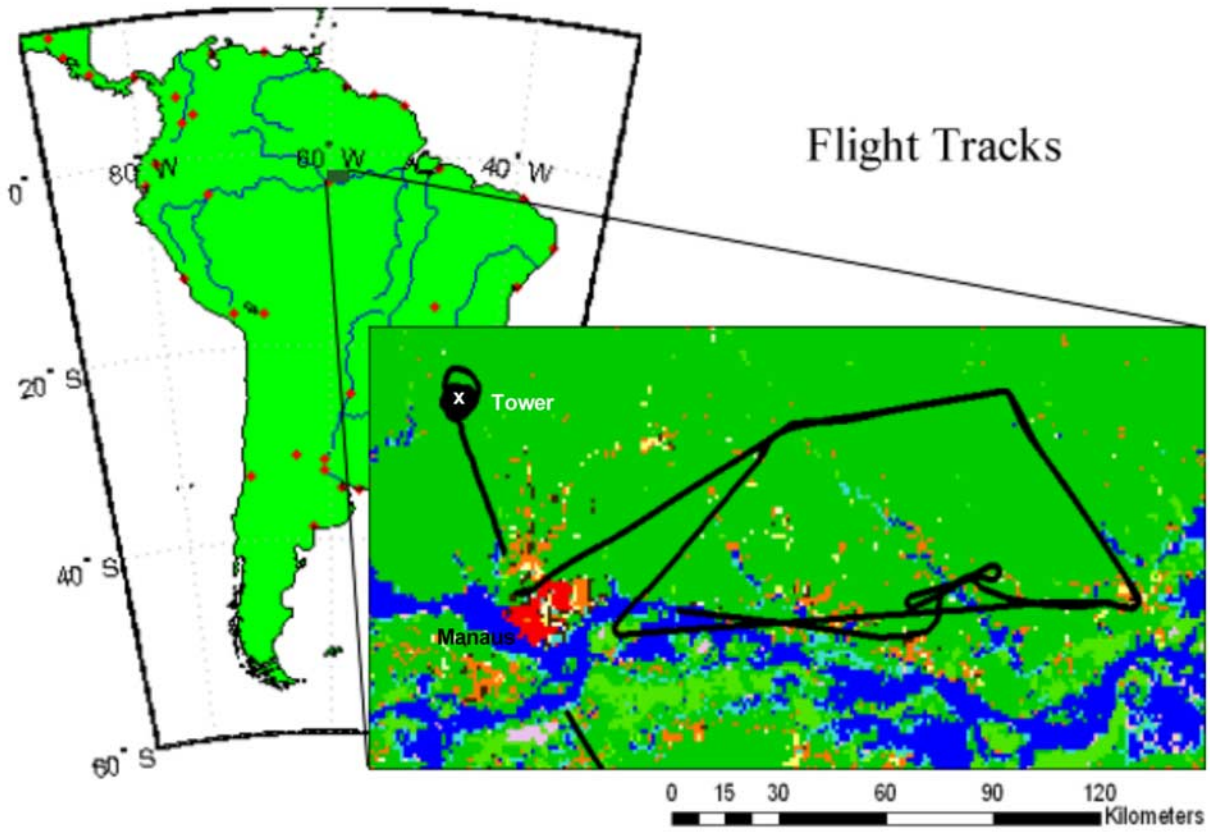

Figure 1. Flight tracks on 6 and 7 September 2004. Tower is drawn at location Z14. Land-use classification: red (city), orange/yellow (urban/agricultural areas), blue (water) and green (forest).

2.2. Analytical VOC Instrumentation

[8] The proton transfer reaction mass spectrometry (PTR-MS) has been described in detail elsewhere [*de Gouw et al.*, 2003; *Hansel et al.*, 1998; *Lindinger et al.*, 2001; *Lindinger et al.*, 1998]. The sensitivity of the PTR-MS instrument during the TROFFEE field study was typically on the order of 70 Hz/ppbv (counts per second per ppbv) for acetone and 50 Hz/ ppbv for methanol at 2.0 mbar buffer gas pressure with a reaction time of 110 μs and 4 MHz H_3O^+ ions. The detection limit (DL) for compounds investigated in this work was inferred from a signal-to-noise ratio (S/N) of 2 according to DL = 2 $\times$ SD_{blank}/sensitivity, with SD_{blank} being the standard deviation of background count rates. For a 5-s (2-s) integration time, this resulted in theoretical detection limits around $\sim$20 pptv ($\sim$58 pptv). We used a gravimetrically prepared multicomponent VOC standard to calibrate the PTR-MS instrument for methanol, acetonitrile, acetone, acetaldehyde, benzene, toluene, isoprene, methyl-vinyl-ketone (MVK), and camphene with an estimated uncertainty of $\pm$15%.

[9] Gas chromatography-mass spectrometric (GC-MS) samples were stored at approximately -30°C until analysis at National Center for Atmospheric Research (NCAR) Boulder laboratory, except during transit from Brazil to USA, when they were at ambient temperature for approximately 1 day. They were desorbed thermally using an NCAR-made system [*Greenberg et al.*, 1994] and analyzed by gas chromatography with mass spectrometric detection (model 5890 gas chromatograph, model 5972 mass selective detector, Hewlett-Packard, Palo Alto, CA). Details of the analysis are given in the work of *Greenberg et al.* [2004].

[10] Setup and operation of the airborne Fourier Transform Infra Red (FTIR)-instrument are described in detail by *Yokelson et al.* [1997]. Briefly, the system consisted of an infrared spectrometer (Michigan Digital Automatic Computer (MIDAC), Inc. model 2500; used at 0.5 cm^{-1} resolution), a White cell (IR Analysis, Inc.), an IR detector, and transfer optics, which were all co-mounted on an aluminum, optical table (Newport, Inc.; 28 $\times$ 175 $\times$ 11 cm^3) shock-mounted (Aeroflex, Inc.) to the floor of the aircraft. For ambient air samples collected on the research aircraft, a portion of the flow through the FTIR cell was diverted to fill canister samples that were later analyzed at University of California, Irvine (UCI) using gas chromatography/flame ionization detector (GC/FID), gas chromatography/mass spectrometry (GC/MS), and gas chromatography/electron capture detector (GC/ECD). Isoprene samples collected in canisters during the research flights based out of Manaus showed good agreement with PTR-MS measurements (PTR-MS/GC-FID: 1.13, R^2: 0.96), suggesting minimal interference due to the presence of other VOCs (such as methyl butenols and methyl butanals) that could exhibit the PTR-MS mass channel M/Z 69^+ [*Fall et al.*, 2001].

2.3. Flux Methods

[11] A detailed description of the experimental setup for ground-based eddy covariance (EC) and disjunct eddy covariance (DEC) measurements using the PTR-MS instrument has been described elsewhere [*Karl et al.*, 2001, 2002, 2004; *Rinne et al.*, 2001; *Spirig et al.*, 2005]. Briefly, ground-based fluxes were measured using a PTR-MS instrument by scanning through eight important ions corresponding to the most prominent biogenic VOCs (isoprene, monoterpenes, methanol, acetone and acetaldehyde), tracer compounds (i.e., acetonitrile for biomass burning influence) and oxidation products of isoprene chemistry (methyl-vinyl-ketone (MVK) and methacrolein (MAC)). Count rates on each mass channel were accumulated for 0.1 s (isoprene and monoterpenes), 0.2 s (methanol, acetone, and MVK + MAC), and 0.5 s (acetonitrile and acetaldehyde). Delay times through sampling lines were calculated based on the covariance between isoprene and vertical wind velocity, measured by a 3D sonic anemometer (R2, Gill Instruments, UK).

[12] The mean Mixed Layer Gradient (MLG) approach has been extensively used for airborne VOC flux measurements in the mixed layer [*Greenberg et al.*, 1999a; *Helmig et al.*, 1998; *Spirig et al.*, 2004] and is based on large eddy simulations (LESs) [*Patton et al.*, 2001; *Wyngaard and Brost*, 1984]. In general, two approaches are used. The most common, the MLG method, relates the surface (F_s) and entrainment (F_e) fluxes to the measured concentration gradient (dC/dz) in the mixed layer (ML) according to:

$$\frac{\partial C}{\partial z} = -g_b(z/z_i)\cdot\frac{F_s}{z_i w^*} - g_t(z/z_i)\cdot\frac{F_e}{z_i w^*} \tag{1a}$$

where C is the concentration, F_s is the surface flux, F_e is the entrainment flux, z is the measurement height, z_i is the height of the PBL, w^* is the convective velocity scale, and g_b and g_t are analytical functions obtained from LES models.

[13] The g_b and g_t functions were adopted from *Patton et al.* [2001], who explicitly calculated these analytical functions over a forest:

$$\begin{aligned} g_b &= 0.75\cdot(z/z_i)^{-0.8} \\ g_t &= 0.7\cdot(1-z/z_i)^{-2} \end{aligned} \tag{1b}$$

[14] The second approach, the MLV method, relates the variability (standard deviation) of a quantity (i.e., concentration) with its surface and entrainment flux. The variance (σ_C^2) is parameterized using convective scaling as follows:

$$\sigma_C^2 = \left(\frac{F_e}{w^*}\right)^2 f_t(z/z_i) + \left(\frac{F_s}{w^*}\right)^2 f_b(z/z_i) + 2\cdot\left(\frac{F_e F_s}{w^{*2}}\right) f_{tb}(z/z_i) \tag{2a}$$

$$f_t(z/z_i) \cong 3.1\cdot(1-z/z_i)^{-2/3} \tag{2b}$$

$$f_b(z/z_i) \cong 1.5\cdot(z/z_i)^{-3/5} \tag{2c}$$

$$f_{tb}(z/z_i) = 0.5\cdot(f_t f_b)^{1/2} \tag{2d}$$

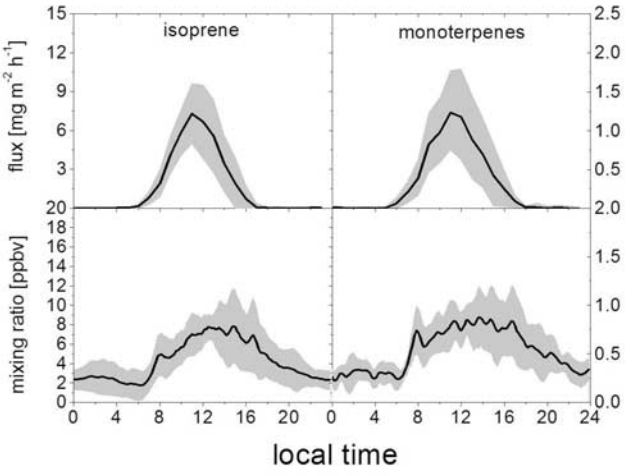

Figure 2a. (a) Isoprene (left panel) and monoterpene (right panel) fluxes (top panels) and mixing ratios (bottom panel) measured on the ground at Z14 between 14 and 29 September 2004. Light-dependent monoterpene emissions result in a pronounced diurnal flux and mixing ratio cycle. Black lines represent the study mean and gray area represents the standard deviation.

The convective velocity scale is commonly calculated from the sensible heat flux ($w'T'$), temperature (T), gravitational constant (g), and the boundary layer height (z_i):

$$w^* \equiv \left(\frac{g}{T}\overline{w'T'}z_i\right)^{1/3} \tag{3}$$

The convective velocity scale was based on turbulence measurements conducted on the ground at Z14. The MLV method requires fast concentration measurements and a sampling rate of ideally >10 Hz. Due to the lack of fast sensors, the variance method had not been used for VOC measurements previously. *Lenschow et al.* [1999] theorized that the 10-Hz sampling requirement could be relaxed, for example, down to 0.01–0.03 Hz, if various scaling arguments are used. However, in order to use a slower sampling rate, accompanying 10-Hz eddy covariance measurements of another quantity (i.e., H_2O) would be needed. In the present study, we used a 10-Hz sampling rate and acquired VOC concentrations at a disjunct sampling interval of 1 s. White noise due to Poisson counting statistics (standard deviation of the background counting statistics) was subtracted from the true geophysical standard deviation.

3. Results and Discussion

3.1. Surface Fluxes and Mixed Layer Gradients Measured at Z14

3.1.1. Surface Fluxes Measured by Eddy Covariance

[15] Figure 2a summarizes the ground-based flux and mixing ratio measurements. The whole range of noontime isoprene and total monoterpene fluxes (upper panels) covered values between 1.5 and 12 mg/m^2/h and between 0 and 2.5 mg/m^2/h, respectively. Noontime (12:00 to 14:00 local time (LT)) temperature and radiation conditions ranged between 28 and 32°C and between 800–1600 PAR, respec-

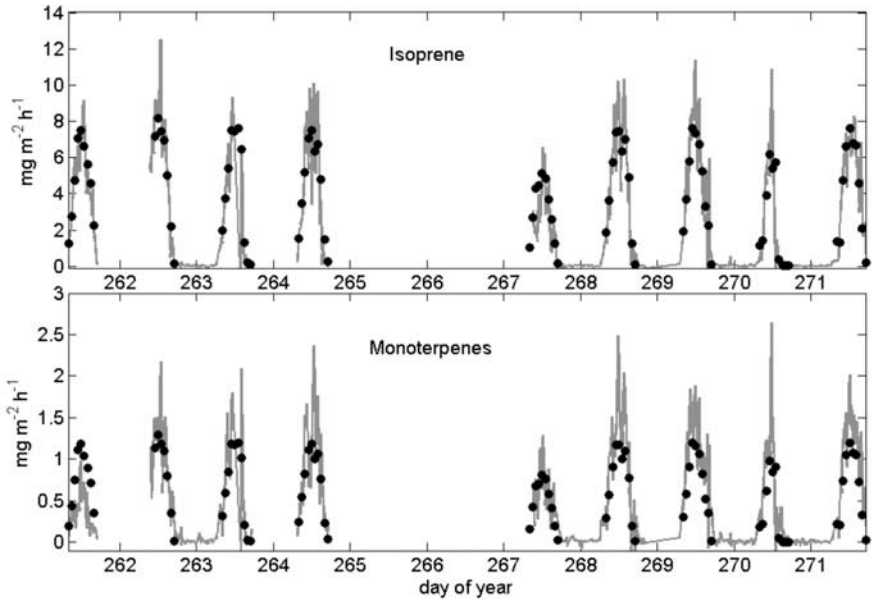

Figure 2b. Isoprene and monoterpene fluxes measured on the ground (gray) compared with the emission model MEGAN (black dots).

tively. Nighttime temperatures were between 18 and 24°C. The study average isoprene flux was centered around 7.8 ± 2.3 mg/m^2/h at local noon. The study average monoterpene flux showed a pronounced diurnal cycle similar to isoprene suggesting light- and temperature-dependent emissions peaking at 1.2 ± 0.5 mg/m^2/h at local noon. This has also been observed in plant enclosure measurements [*Kuhn et al.*, 2004]. These fluxes can be predicted by light- and temperature-dependent algorithms of the G95 [*Guenther et al.*, 1995] and G06 [*Guenther et al.*, 2006] emission models. We used the new emission model MEGAN [*Guenther et al.*, 2006] which was parameterized with five canopy layers and constrained by a leaf area index of 6 m^2/m^2. The emission model MEGAN predicted measured latent and sensible heat fluxes using its standard parameterization [*Guenther et al.*, 2006], but overestimated these by 10%. However, slightly higher sensible and latent heat fluxes had little effect on calculated leaf temperatures and thus isoprene and monoterpene emission rates. A day by day comparison of measured isoprene and monoterpene with the MEGAN emission model is shown in Figure 2b. The model-measurement comparison demonstrates that light and temperature variations account for most of the isoprene and monoterpene emission variation. Model predictions are depicted for isoprene (R^2: 0.80; slope model/measurement: 0.92) and total monoterpene (R^2: 0.78; slope model/measurement: 0.88) fluxes. The black dots represent the model output calculated with standard MEGAN model fitting parameters [for more detail, see: *Guenther et al.*, 2006] (c_{t1} = 95; c_{t2} = 230; T_{opt} = 313; c_{l1} = 1.016, c_{l2} = 0.004 − 0.0005 × log(mean(max(SunPPFD)) × 0.25), with SunPPFD being the fraction of leaves exposed to full sunlight and E_{opt} = 2). Canopy-scale basal emission rates at standard conditions (30°C, 1000 PAR) for the ground site were calculated to be 5.9 ± 0.1 mg/m^2/h for isoprene and 1.2 ± 0.1 mg/m^2/h for total monoterpene fluxes. Surface measurements demonstrate that light and temperature are the main driving variables for isoprene emissions on timescales considered during this study. We will take these temperature and light variations into account when comparing ground-based fluxes to airborne profiles obtained 1 week prior to the ground-based study (next section).

3.1.2. VOC Mixing Ratios

[16] Mean noontime isoprene mixing ratios (Figure 2a, lower panel) were 7.8 ± 3.7 ppbv with peak values up to 15 ppbv. Table 1 summarizes isoprene and total monoterpene concentrations measured in the surface and mixed layer in the Amazon Basin over the last two decades. Our ground-based isoprene mixing ratios are somewhat higher than what has been observed over Surinam during the Cooperative LBA Airborne Regional Experiment 2001 (LBA-CLAIRE-2001) campaign during the wet season [*Warneke et al.*, 2001; *Williams et al.*, 2001]. In Rondonia, *Kesselmeier et al.* [2002] observed higher isoprene emissions during the dry season than the wet season, which would be consistent with these observations. *Warneke et al.* [2001], for example, reported isoprene mixing ratios in the range of 0.5–12 ppbv. Low isoprene mixing ratios were attributed to the marine influence of air masses advected over Surinam. During flight legs that sampled air close to the Brazilian border, isoprene mixing ratios were measured up to 7 ppbv (mean: ~3.3 ppbv), close to what we observed during the TROFFEE flights. *Helmig et al.* [1998] observed 3.2 ppbv isoprene in the Peruvian Amazon on the ground. At a site close to Manaus (Z2, Ducke reserve), *Rasmussen and Khalil* [1988] reported mean isoprene mixing ratios of 3 ppbv at the ground. At the same site, *Greenberg and Zimmerman* [1984] measured 2.4 ppbv and *Zimmerman et al.* [1988] measured 5.5 ppbv. Lower isoprene mixing ratios could reflect seasonal or ecosystem related differences.

[17] The mean isoprene mixing ratio observed in the mixed layer (ML) (i.e., 600 m above ground) during this study was 5.2 ppbv, comparable to results obtained by

Table 1. Comparison of VOC Mixing Ratio Measurements (ppbv) in the Amazon From Different Studies

Location[a]	Season	Landscape	ISO[b]	MT[c]	MeOH	Acetone	Acetaldehyde	MVK + MAC	References[d]
SL, A, BR	Dry	Forest	2.4	0.51	–	–	–	–	G1984
SL, A, BR	Dry	Forest	5.5	0.34	–	–	–	–	Z1988
SL, A, BR	Wet	Forest	2.3	0.23	–	–	–	–	Z1988
SL, A, BR	Wet	Forest	∼3	–	–	–	–	–	R1988
SL, N.E.V.	Wet	Forest	1.6	–	–	–	–	–	D1996
SL, S.E.V.	Wet	Forest	3.3	–	–	–	–	–	D1996
SL, C.V.	Wet	Savanna	2.2	–	–	–	0.35	–	S1996
SL, N. Peru	Wet	Forest	3.3	0.21	–	–	–	1.24	H1998
SL, F. Guiana	Wet	Forest	1.8	0.24	–	–	–	–	PC[e]
SL, A, BR	Wet	Forest	∼6	∼0.6	–	–	–	∼3	Ke2000
SL, R., BR	Wet	Forest	∼5	∼0.6	–	∼1	∼0.4	∼1	Ke2002
SL, R., BR	Dry	Forest	∼12	∼0.4	∼3	∼0.3	∼3	∼3.6	Ke2002
SL, C.V.	Wet	Savanna	1.6	–	–	–	–	1.0	Ho2002
SL, C.V.	Dry	Savanna	0.8	–	–	–	–	0.4	Ho2002
SL, N.E.V.	Dry	Savanna	0.5	–	–	–	–	0.3	Ho2002
SL, A, BR	*Dry*	Forest	7.8	0.87	4.1	2.2	1.2	2.1	This study
ML, A, BR	Dry	Forest	2.3	–	–	–	–	–	G1984
ML, Guyana	Wet	Forest	∼2	–	–	–	–	–	Gr1986
ML, A, BR	Wet	Forest	∼1.5	–	–	–	–	–	R1988
ML, A, BR	Wet	Forest	1.8	0.17	–	–	–	–	Z1988
ML, N. Peru	Wet	Forest	1.4	0.06	–	–	–	0.87	H1998
ML, Surinam	Wet	Forest	–	<0.3	1.1	2.9	1.7	–	Wi2001
ML, Surinam	Wet	Forest	∼3.3	–	4	–	–	2.5	Wa2001
ML, R, BR	Wet	Pasture	1.7	0.09	–	–	–	–	G2004
ML, R, BR	Wet	Forest	6.7	0.69	–	–	–	–	G2004
ML, A, BR	Wet	Forest	2.3	0.2	–	–	–	–	G2004
ML, A, BR	Wet	Forest	2.1	0.25	–	–	–	–	G2004
ML, A, BR	Wet	Forest	2.9	0.21	–	–	–	–	G2004
ML, Para, BR	Wet	Forest	0.6	0.08	–	–	–	–	G2004
ML, A, BR	Dry[f]	Forest	∼1.7	∼0.09	–	–	–	∼0.5	Ku2007
ML, A, BR	*Dry*	Forest	5.5	0.52	3.5	2.2	1.5	2.3	This study

Values are typically average observed mixing ratios during daytime. Exact times of sample collection are often not available and therefore not reported.

[a]Location: SL, A, BR: Surface Layer, Amazonas, Brazil; SL, N.E.V.: Surface Layer, N.E. Venezuela; SL, S.E.V.: Surface Layer, S.E. Venezuela; SL, C.V.: Surface Layer, C. Venezuela; SL, N. Peru: Surface Layer, N. Peru; SL, F. Guiana: Surface Layer, French Guiana; SL, R., BR: Surface Layer, Rondonia, Brazil; ML, A, BR: Mixed Layer, Amazonas, Brazil; ML, Guyana: Mixed Layer, Guyana; ML, N. Peru: Mixed Layer, N. Peru; ML, Surinam: Mixed Layer, Surinam; ML, R, BR: Mixed layer, Rondonia, Brazil; ML, Para, BR: Mixed Layer, Para, Brazil.

[b]Isoprene.

[c]Monoterpenes.

[d]References: G1984: [*Greenberg and Zimmerman*, 1984]; Z1988: [*Zimmerman et al.*, 1988]; R1988: [*Rasmussen and Khalil*, 1988]; D1996: [*Donoso et al.*, 1996]; S1996: [*Sanhueza et al.*, 1996]; H1998: [*Helmig et al.*, 1998]; Ke2000: [*Kesselmeier et al.*, 2000]; Ke2002: [*Kesselmeier et al.*, 2002]; Ho2002: [*Holzinger et al.*, 2002]; Gr1986: [*Gregory et al.*, 1986]; Wi2001: [*Williams et al.*, 2001]; Wa2001: [*Warneke et al.*, 2001]; G2004: [*Greenberg et al.*, 2004]; Ku2007: [*Kuhn et al.*, 2007].

[e]J. Greenberg [personal communication].

[f]Early dry season/end of wet season.

Warneke et al. [2001] in the southern part of Surinam during the LBA-CLAIRE-2001 (3.3 ppbv). *Greenberg et al.* [2004] also reported mixed layer isoprene mixing ratios at various tropical forest sites. While observations up to 2.9 ppbv in Balbina (approximately 50 km east of Z14) and up to 6.7 ppbv in Jaru (Rondonia) are close to what we measured above Z14 (Table 1), the mixed layer mixing ratios measured at Tapajos (Pará) were significantly lower (0.6 ppbv). These differences most likely reflect the spatial and temporal variability of isoprene fluxes in the tropics. Lower isoprene emissions (2.5 mg/m^2/h) in a drought-stressed ecosystem were recently observed in Central America [*Karl et al.*, 2004].

[18] Measured isoprene concentrations summarized in Table 1 range between 0.6 and 6.7 ppbv in the ML and between 0.5 and 12 ppbv in the SL and are all systematically lower than values modeled by state of the art 3D-CT models in this region. In their model runs, *Kuhlmann et al.* [2003] assumed 50% lower isoprene emissions in the tropics than G95, but reported modeled isoprene mixing ratios up to 25 ppbv in the Amazonian PBL. This is 5 times higher than our observations in the mixed layer and 3–4 times higher than our study-averaged surface mixing ratios.

[19] Noontime monoterpene mixing ratios (Figure 2a, lower panel) were 0.8 ± 0.3 ppbv with peak values up to 1.5 ppbv, respectively. The study average monoterpene distribution inferred from GC-MS measurements is shown in Figure 3. α-Pinene, β-pinene and limonene are the most common monoterpenes accounting for 75% of the total. Camphene, α-phellandrene, myrcene, sabinene, and 3-carene were also present in detectable amounts. For comparison, *Andreae et al.* [2002] reported a similar composition of these monoterpenes (α-pinene: 54%, β-pinene: 28%, limonene: 6%) near Manaus at the beginning of the wet season in November 1999.

[20] The presence of these monoterpenes has also been observed in Rondonia [*Kesselmeier et al.*, 2002] at the end of the dry season, but the composition there was dominated by camphene and sabinene contributing >70% to the total monoterpene composition. When modeling atmospheric chemistry, it is important to know the composition of different monoterpenes because of their different reactivities with respect to OH, ozone, and NO_3 and their different secondary aerosol formation potential [e.g., *Griffin et al.*, 1999]. Most regional and global chemistry models still treat

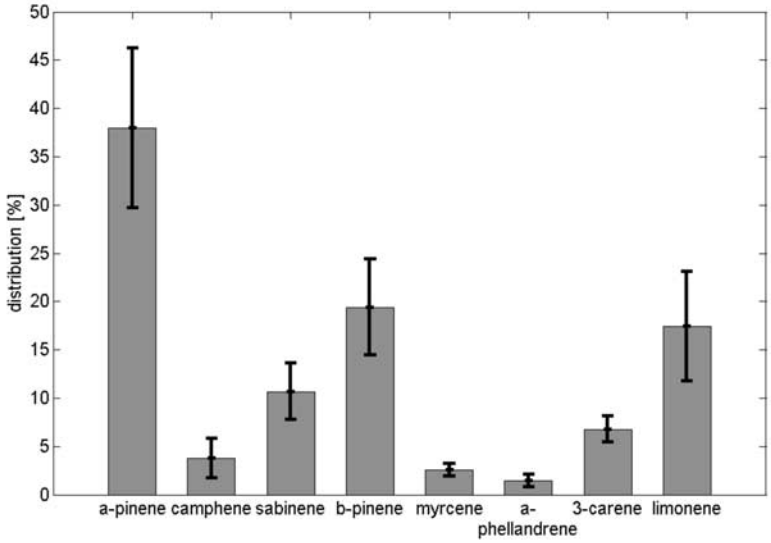

Figure 3. Monoterpene distribution inferred from GC-MS analysis measured at Z14.

monoterpenes as one lumped class of biogenic compounds with properties similar to α-pinene and/or β-pinene. It is therefore valuable to examine the difference with respect to atmospheric reactivity caused by the measured monoterpene composition. For example, based on the composition summarized in Figure 3, we calculate a total effective reaction rate constant with respect to OH (O_3) of 2.5×10^{-10} (1.4×10^{-16}) cm^3/s. Assuming a composition of 50% α-pinene and 50% β-pinene, the weighted reaction rate constant with respect to OH (O_3) would be 6.7×10^{-11} (5.1×10^{-17}) cm^3/s. We applied the weighted reactivity obtained from Figure 3 in our model calculations described in section 3.3. In light of these differences, introducing a reactivity-weighted monoterpene flux in future emission models could help bridge the complexity of ecosystem-specific monoterpene compositions with lumped chemistry schemes deployed in global and regional air-chemistry models.

[21] Table 1 also summarizes other important oxygenated VOCs (OVOCs). Study average noontime mixing ratios of methanol, acetone, acetaldehyde, and MVK + MAC were 4.1, 2.2, 1.2, and 2.1 ppbv in the SL and 3.5, 2.2, 1.5, and 2.3 ppbv in the ML, respectively. While not many measurements of these compounds are available, these mixing ratios are comparable to the few observations reported in other studies.

3.1.3. Mixed Layer Gradient (MLG) and Mixed Layer Variance (MLV)

[22] Compared to plant enclosure measurements, canopy-scale flux (i.e., eddy covariance) measurements have the advantage of integrating over the whole forest stand without the necessity of guessing the species distribution of more than 200 species/ha, common for a tropical rainforest. Canopy-scale measurements, however, can still be biased due to the specific species distribution within the tower footprint (i.e., $\sim$100–3000 m) for the flux measurement. In order to determine the landscape-scale ecosystem flux, we combined tower-based flux measurements with airborne profiling above the measurement tower using the MLG and MLV technique [*Lenschow et al.*, 1999].

[23] In order to test the effect of chemical reactivity on the MLG functions, we assumed a PBL turnaround timescale of $z_i/w^* \sim 10$ min, an upper limit of OH concentrations of 5×10^6 molecules/cm^3, and measured mixed layer ozone mixing ratios of 20 ppbv. The resulting bias for the surface (F_s) and entrainment (F_e) fluxes of isoprene (equation (2)) due to reactive losses was 14 and 13%, respectively.

[24] Two stacks of five circles ($\sim$5 km in diameter) each 6 min long were flown sequentially between 10:00 and 11:30 local time on 6 September. Figure 4a shows the average concentration gradient (all data) for isoprene and monoterpenes together with a fitted profile based on equations (1a)–(1b). The top of the PBL ($z/z_i = 1$) was defined as the bottom of the developing cloud layer and was $\sim$1200 m deep. The depth is close to an average 1100-m-deep boundary layer determined by a climatology at the site [*Fisch et al.*, 2004]. The surface and entrainment fluxes obtained from these profiles are listed in Table 2. Figure 4b shows an example of the variance method for monoterpenes. The left panel shows the variance of the monoterpene concentration plotted for a 20-s interval, averaged over 5 min, as a function of global positioning system (GPS) altitude. The variance of a compound was calculated for 5-, 10-, 20-, and 60-s time intervals. The variance should be calculated for timescales long enough so that the most important eddy spectrum is captured. *Lenschow et al.* [1994] showed how long turbulent quantities should be measured in order to capture the most important time/length scales in the PBL. Here we find that the 20-s interval was sufficient to explain most of the variance. Equation (2) can then be solved graphically for each flight level (right panel). Any suitable combination of surface and entrainment fluxes can explain the variance for each individual flight level. For example, the variance at the lowest flight level (blue) on the left panel is characterized by the steepest slope on the right panel (blue) indicating that this level is more influenced by the surface flux than the entrainment flux. This will change as a function of altitude in the PBL. For example, the red curve at $z/z_i = 0.8$ has the smallest slope. A minimum of two flight legs at two different

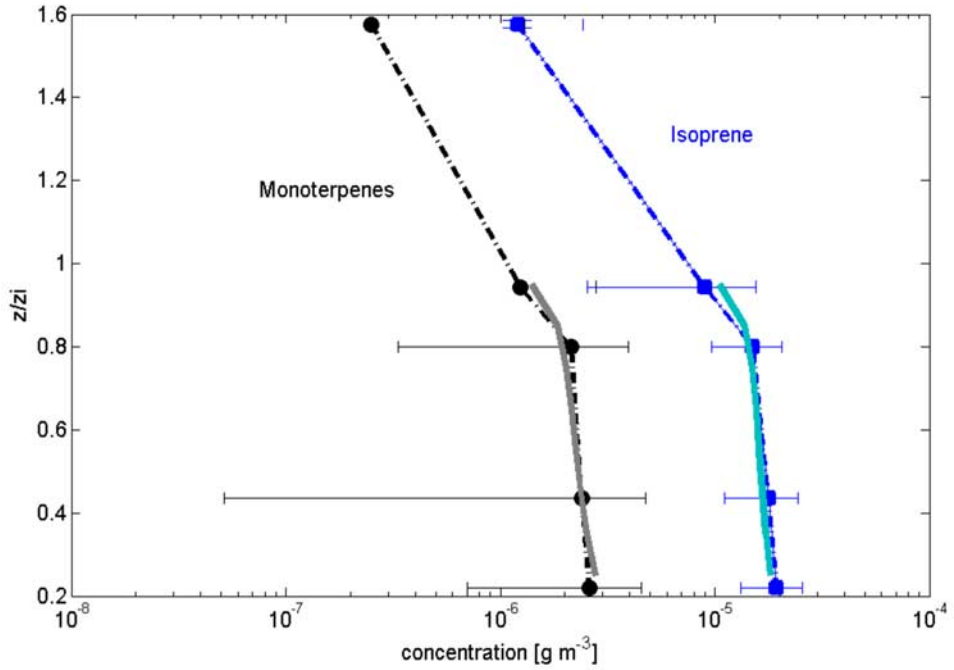

Figure 4a. Mixed layer gradient: Measured concentration of isoprene (blue) and monoterpene (black) concentrations. Solid gray and solid light blue lines represent the gradient fitted according to equations (1a) and (1b); z_i is the height of the PBL.

altitudes is needed to solve equation (2) and calculate a unique surface (F_s) and entrainment (F_e) flux combination. Ideally, all curves intersect at one point which then reflects the surface and entrainment flux at a given time. This might not always be achieved due to experimental variability (i.e., sequentially flown profiles). In our case, the triangle defined by the three intersecting curves would define the experimental uncertainty of the flux calculation. *Lenschow et al.* [1999]

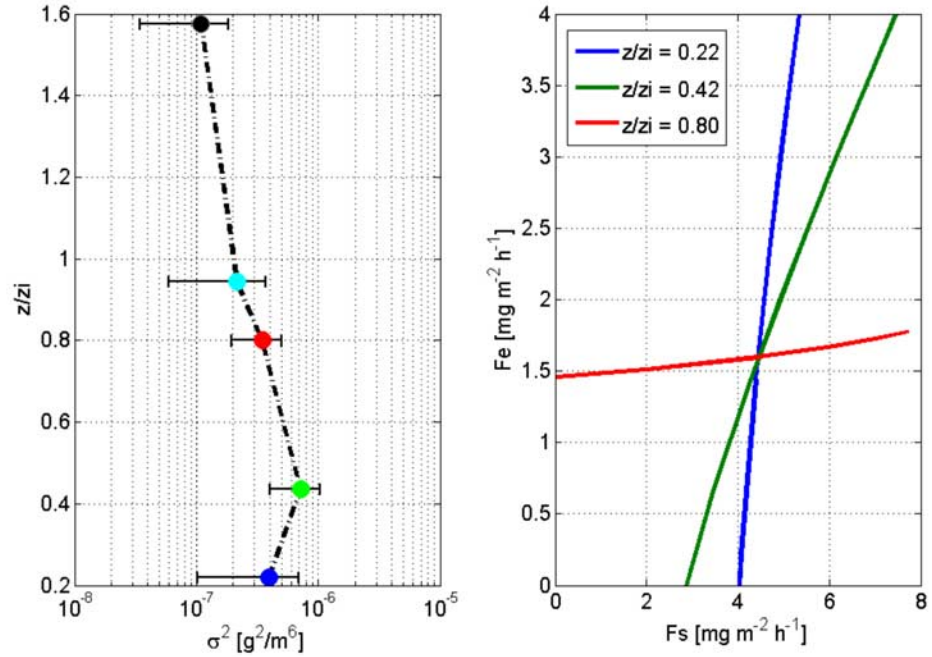

Figure 4b. Left panel: Mixed layer variance of the monoterpene concentration as a function of z/z_i. Right panel: Iteratively solved surface (F_s) and entrainment (F_e) fluxes according to equation (3). Individual profiles are color coded according to the variance calculated for each level.

Table 2. Fluxes Inferred From EC and MLG Methods

Flux units, mg/m^2/h Method	F_s[a] EC	F_s[b] MLG	F_e[b] MLG	F_s[b] MLV	F_e[b] MLV	F_s[b] Average	F_e[b] Average	F_e/F_s, %	v_e, cm/s	C_{ML}, ppbv
Isoprene	8.3 ± 3.1	11.6 ± 4.0	3.6 ± 1.5	12.5 ± 1.0	5.0 ± 0.9	12.1 ± 4.0	4.3 ± 1.5	36	8.5 ± 2.8	5.5 ± 2.6
MT[c]	1.7 ± 1.3	2.5 ± 0.8	0.3 ± 0.13	4.4 ± 1.2	1.1 ± 0.2	3.5 ± 1.2	0.7 ± 0.2	22	10.5 ± 3.0	0.52 ± 0.2

Column 2: Study's average EC surface fluxes (F_s) measured at Z14. Column 3: MLG surface fluxes (F_s) According to equations (1a) and (1b) on 6 September. Column 4: MLG entrainment fluxes (F_e) According to equations (1a) and (1b) on 6 September. Column 5: MLV surface fluxes (F_s) according to equations (2a)–(2d) on 6 September. Column 6: MLV entrainment fluxes (F_e) according to equations (2a)–(2d) on 6 September. Column 7: Mean MLG surface flux (F_s). Column 8: Mean MLG entrainment flux (F_e). Column 9: Ratio between entrainment and surface flux (F_e/F_s). Column 10: Entrainment velocities (v_e). Column 11: Mixed layer mixing ratios (C_{ML}).

[a]Corrected for environmental conditions accounted during profile flights.

[b]Not corrected for chemical bias (upper limit of chemical bias would yield 14% lower fluxes).

[c]Monoterpenes.

report on the influence of mesoscale variability due to cumulus clouds. Our isoprene variance is larger (i.e., ~3–5 times) than the dimethyl sulfide (DMS) variance over the ocean and mesoscale variability in the mixed layer plays a significantly smaller role. However, our measurements show that the variance technique cannot be applied close to the top of the PBL (i.e., $z/z_i > 0.9$). This is most likely caused by increased variability due to cumulus clouds. In addition, the functional dependence of the top down function f_t becomes very large as z/z_i approaches 1. For these reasons, the variance calculated close to the top of the PBL (light blue) is prone to large errors and was thus omitted from the graphical analysis.

[25] Table 2 summarizes results obtained from the MLG and MLV calculations. The average surface flux for isoprene using equations (1a)–(1b) was 11.6 ± 4.0 mg/m^2/h. For comparison, the variance method (equation (2)) yielded 12.5 ± 1.0 mg/m^2/h. Airborne and ground-based measurements were made with the same instrument and so were conducted on consecutive days. Therefore we compare the light- and temperature-corrected surface flux calculated for the whole study (section 3.1.1) with flux measurements calculated from the airborne profile measurements on 6 September 2004. While temporal variation in VOC emissions cannot be excluded, it is noted that meteorological conditions (such as *cumulus humilis* development in the late morning) remained fairly constant throughout the study and that light and temperature variations have been taken into account. Column 2 lists the surface flux measured on the ground using the eddy covariance technique (8.3 ± 3.1 mg/m^2/h). Taking upper limits of the chemical reactivity into account, MLG fluxes would be up to 14% smaller, i.e., 10.6 ± 3.8 mg/m^2/h for isoprene. Surface and MLG fluxes would then agree within ~20%. Because this chemical bias represents an upper limit, we do not correct values listed in Table 2. One main consideration when comparing ground-based fluxes with airborne fluxes arises from the fact that both represent a different flux footprint. Thus we believe that airborne measurements are a very useful step in scaling biogenic emissions up to a regional scale. With this in mind, we argue that mean isoprene MLG and MLV fluxes are within the range of fluxes calculated using the eddy covariance technique. Some differences might as well originate from the assumptions inherent to the methods used. The good agreement suggests that these methods are within the expected uncertainty. In comparison, the difference for monoterpene fluxes is somewhat bigger than for isoprene and could suggest other contributions to the variability (i.e., higher spatial variation of these emissions). Columns 9 and 10 list entrainment fluxes which were calculated to be on the order of 20–40% of surface emissions between 10:00 and 12:00 local time. The inferred entrainment velocities (Column 10) are on the order of 8.5–10.5 cm/s. In comparison, entrainment above other landscapes has been reported to be about 5 cm/s [*Stull*, 1988]. *Baumann et al.* [2000] indicated that entrainment is still very uncertain in many models (i.e., up to 2 orders of magnitude). *Faloona et al.* [2005] reported entrainment rates up to 1 cm/s over a stratocumulus-topped ocean atmosphere. Over land, unstable conditions are expected to result in higher entrainment rates; however, measurements are very scarce. An LES study by *Patton et al.* [2005] suggested entrainment rates of ~2 cm/s under neutral conditions. Convection and transport through clouds can also transport PBL air vertically. *Albrecht et al.* [1985], for example, observed a convective mass flux expressed as a velocity up to 10 cm/s.

3.1.4. PBL Budget–Mixed Box Technique

[26] Surface emissions can also be used in a simple budget analysis. The surface and entrainment fluxes are related to the lifetime of a compound according to:

$$F_s - F_e = (k_{OH} \cdot [OH] + k_{O_3} \cdot [O_3]) \cdot C_{average} \cdot z_i, \qquad (4)$$

where F_s is the surface flux, F_e is the entrainment flux, k_{OH} is the rate constant with respect to OH, k_{O_3} is the rate constant with respect to O_3, $C_{average}$ is the average PBL concentration, z_i is the height of the PBL, [OH] is the OH concentration, and [O_3] is the ozone concentration.

[27] Here we use equation (4) to calculate the lifetime (OH concentrations) that would be necessary to reproduce the observed VOC mixing ratios in the PBL based on fluxes inferred from the ML observations. We use a k_{OH} of 1×10^{-10} cm^3/s and a k_{O_3} of 1.3×10^{-17} cm^3/s for isoprene and neglect the reaction with NO_3, which is expected to be small during daytime. ML ozone mixing ratios were 10 ppbv; the F_e/F_s ratio (0.3) was adopted from the MLG and MLV observations. The average OH concentration calculated according to equation (4) using ML isoprene fluxes from Table 2 yields $1.3 \pm 0.5 \times 10^6$ molecules/cm^3. For monoterpenes, we calculate an OH concentration of $1.7 \pm 1.0 \times 10^6$ molecules/cm^3.

3.2. Land-Use Change

[28] Among the big unknowns in estimating regional landscape fluxes in the tropics are uncertainties in assigning VOC emission potentials to different ecoregions. Biogenic

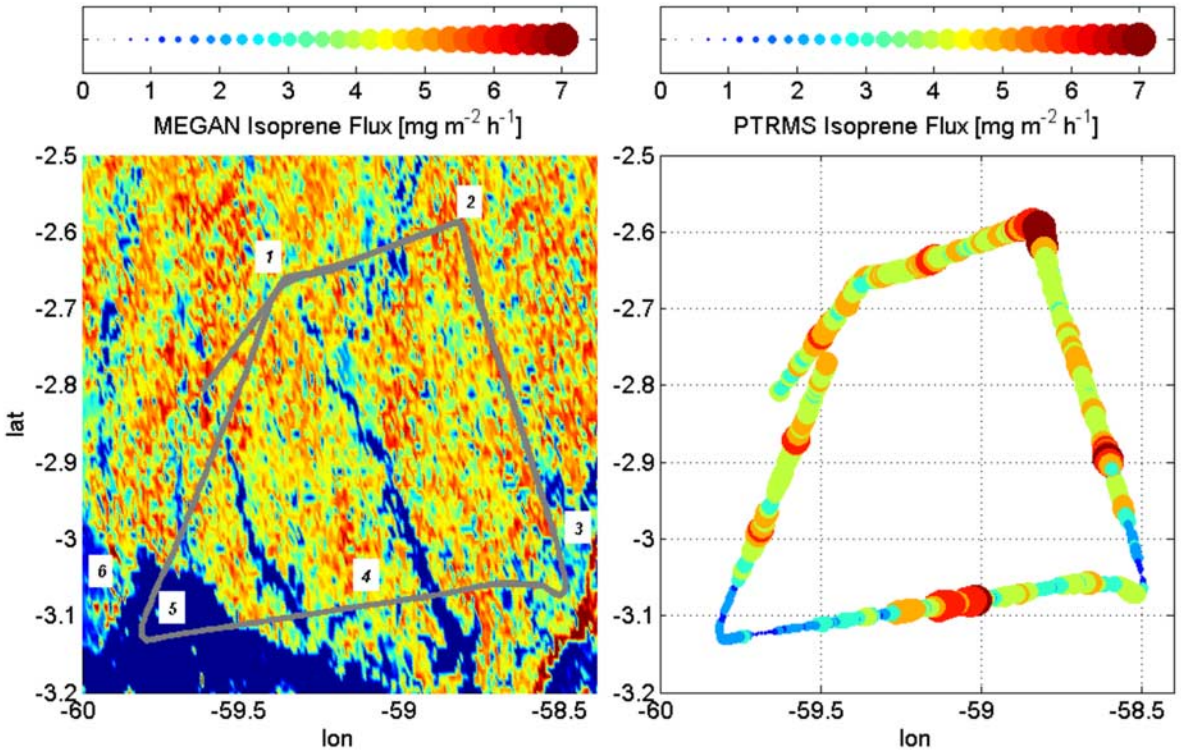

Figure 5. Isoprene emission map generated for flight conditions (34°C, 1260 PAR) from MEGAN (left panel) compared to measurements using the MLV techniques (right panel). The gray line on the left panel depicts the flight track. Numbers 1–6 on the left panel indicate different land cover types: (1) mixed forest/plantation, (2) primary tropical forest, (3) soybean plantations, (4) mixed forest/plantation, (5) water, (6) urban (Manaus).

emission measurements from tropical ecosystems are scarce due to logistical problems and almost entirely confined to a few accessible primary forest locations. Uncertainties of satellite land cover data, satellite-derived vegetation area index data and land cover change due to agricultural expansion and deforestation further complicate the assignment of VOC emission potentials over different landscapes [*Guenther et al.*, 2006]. Here we extended our airborne measurements by flying a racetrack pattern north east of Manaus on 7 September 2004. The airplane flew along a constant altitude of 675 m above sea level (asl) starting at 10:00 local time. The racetrack was repeated twice and covered various landscapes (primary forest, mixed water/forest, soybean plantations, and mixed agricultural plantations). The total leg length (~320 km) was chosen such that it could be repeated after 1.5 h. Figure 5 (left panel) depicts the isoprene emission map calculated from MEGAN for flight conditions (34°C and 1260 PAR). On top of the emission map, we plotted the flight plan in gray. The right panel shows the surface flux calculated using equation (2) and parameters (F_e/F_s = 0.3) obtained from the airborne profile measurements conducted on the previous day. The convective velocity scale was calculated from ground-based measurements at Z14. The VOC variability was calculated for a 60-s running average. While there is some uncertainty due to assumptions imposed by the MLV technique (i.e., entrainment), the calculated values compare well with the stacked profiles measured above Z14 one day earlier on 6 September 2004. As can be seen in Figure 5, the qualitative agreement between model and measurements is reasonable. Areas indicated by numbers in Figure 5 (left panel) are based on different land cover information: (1) mixed forest/plantation, (2) primary tropical forest, (3) soybean plantations, (4) mixed forest/plantation, (5) water, and (6) urban. The isoprene emission potential assignment of MEGAN is compared with measurements in Figure 6 which shows a regression between the model and measurements for isoprene. The fact that we observe a tight linear correlation between the two (R^2 = 0.99) is encouraging and shows that basic land cover features used in MEGAN are reproduced well. The MEGAN emission map was corrected for the actual environmental conditions (T = 34°C and 1260 PAR) in order to quantitatively compare with flux estimates based on the variance method. The MEGAN isoprene emission estimates are ~40% lower (slope: 0.6) than our observations. This suggests that the MEGAN isoprene estimates are correct for this region within the stated model uncertainty (50%), but also that the estimates may be a lower rather than an upper limit at least for the given ecoregion. Our observations contrast most modeling studies, which assume the opposite (that is, up to 50% reduced isoprene emissions compared to G06 or G95) [*Kuhlmann et al.*, 2003]. Biogenic emissions incorporated in these large-scale chemical-transport models may therefore be too low: even while overestimating biogenic VOC concentrations.

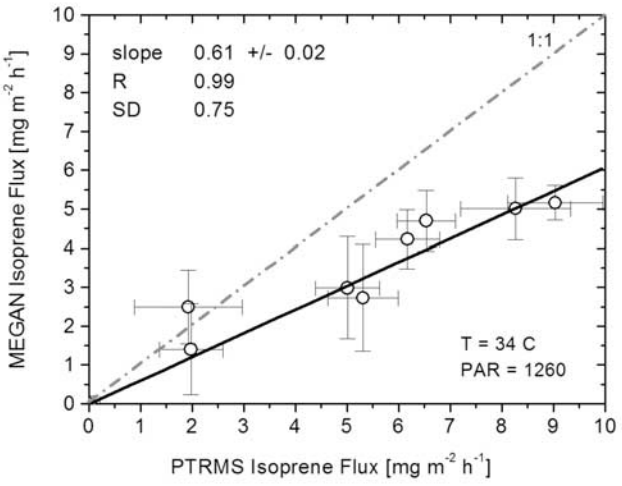

Figure 6. Isoprene fluxes calculated from MEGAN plotted vs. MLV isoprene fluxes for 34°C, 1260 PAR.

3.3. Atmospheric Chemistry of Reactive Biogenic VOCs Above Z14

[29] Isoprene accounts for more than 70% of the total VOC reactivity with respect to OH based on measurements by PTR-MS (VOCs), FTIR (CO and methane), and whole air sampling in combination with GC-MS (VOCs). Other species contributed lower amounts, i.e., CO: 2.2%, CH_4: 1.6%, CH_3OH: 0.4%. Isoprene is therefore one of the most reactive VOCs in the remote tropical atmosphere in the absence of biomass burning. MVK and MAC are thought to be exclusively produced by the reaction of isoprene with oxidants (OH and O_3), with OH being the main oxidant during daytime. These carbonyls have been used in previous studies [*Apel et al.*, 2002; *Holzinger et al.*, 2002; *Warneke et al.*, 2001] to estimate the oxidative fate of isoprene. Figure 7 (left panel) shows the vertical distribution of the (MVK + MAC) to isoprene ratio measured above Z14 on 6 September 2004. The lines aligned with the *x* axis between 1200 and 1900 m indicate the cloud layer due to *cumulus humilis*. The gray (black) solid line shows the mean (median) ratio fitted through all data points collected between 10:00 and 11:30 local time. The ratio is significantly enhanced in the cloud layer. Three processes could explain this increase: (1) isoprene-depleted (older) air from the free troposphere is entrained and (2) the photochemical age increases at higher altitude. While (2) can probably explain part of the increase (that is, the ratio increases from 0.39 at ~300 m to 0.61 at ~1000 m), the drastic change in the CL by a factor of ~4 (from ~0.61 below 1200 m to the theoretical upper limit (~1.2) at ~1800 m above sea level)

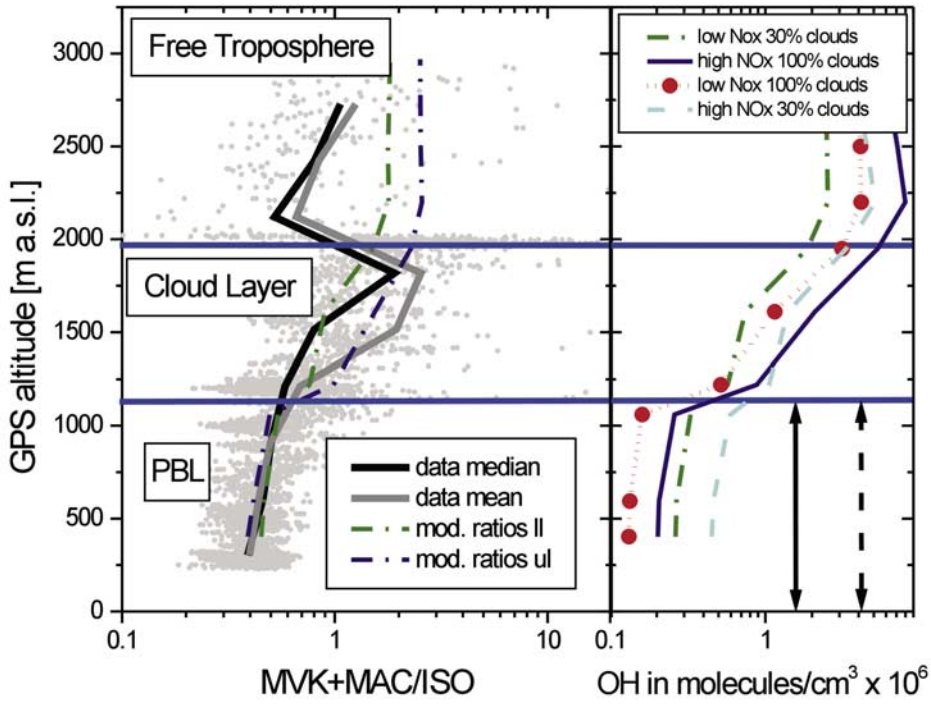

Figure 7. Left panel: (MVK + MAC)/isoprene ratio derived from measurements plotted vs. GPS altitude. The black line corresponds to the median and the dotted gray line to the mean for all data. The dashed green and blue lines represent lower and upper limits of modeled ratios. Right panel: Lower (180 pptv NO_x and 30% cloud cover, green dashed line) and upper (320 pptv NO_x and 100% cloud cover, dark blue solid line) CL limits of modeled OH density plotted as a function of GPS altitude. Also shown are 180 pptv NO_x and 100% cloud cover (red dotted line) as well as 320 pptv NO_x and 30% cloud cover (light blue dashed line) cases. Black solid line with arrows is the calculated OH density according to equation (4) and the black dashed line with arrows is the calculated OH density according to equation (5). Horizontal (aligned with *x* axis) blue lines indicate the depth of the cloud layer.

Table 3. Box Model Simulations

	30%		Clouds	No		Clouds
NO_x emission flux, molecules/cm^2/s	NO_x, ppbv	O_3, ppbv	OH, molecules/cm^3	NO_x, ppbv	O_3, ppbv	OH, molecules/cm^3
2.00e + 09	0.09	10.4	1.60e + 05	0.06	10.0	2.30e + 05
4.00e + 09	**0.18**	**16.2**	**3.93e + 05**	**0.12**	**17.6**	**6.30e + 05**
8.00e + 09	**0.32**	**26.3**	**9.73e + 05**	**0.22**	**29.1**	**1.71e + 06**
1.60e + 10	0.56	39.8	2.30e + 06	0.39	45.0	4.40e + 06
3.20e + 10	0.99	56.9	5.40e + 06	0.66	65.0	8.70e + 06
6.40e + 10	1.70	73.0	9.30e + 06	1.00	84.7	1.33e + 07
1.28e + 11	3.81	78.9	1.27e + 07	1.72	102.0	1.91e + 07

[a]The calculated NO_x, O_3 mixing ratios and OH densities are listed for different NO_x emission scenarios for 30% cloud cover and no clouds. Highlighted in bold are the two scenarios that reproduced measured O_3 best.

is likely also caused by (3) a change of the oxidizing power of the atmosphere. This is supported by the fact that the ratio in the FT (>2000 m) is lower than in the CL.

[30] To test this hypothesis, we initialized a zero-dimensional box model with two setups. First: the NCAR Master Mechanism (MM) [*Hauglustaine et al.*, 1996; *Madronich and Calvert*, 1990] was initiated at standard conditions including basic hydrocarbon chemistry encountered in the Amazon [*Greenberg and Zimmerman*, 1984; *Jacob and Wofsy*, 1988]. CO and methane were measured by FTIR, and VOCs were measured by GC and PTR-MS. NO emissions from soil were incorporated for various emission scenarios listed in Table 3. The planetary nighttime boundary layer height was taken as 0.2 km, ramping up to 1.2 km between 08:00 and 10:00 LT and decreasing back to 0.2 km between 17:00 and 20:00 LT. Entrainment velocities obtained from the mixed layer gradients were incorporated as a first-order rate constant.

[31] Since we did not have NO_x instruments that were able to measure below 1 ppbv, we performed a sensitivity study using various NO_x emission rates that were measured from tropical soils in the Amazon [*Kaplan et al.*, 1988; *Torres and Buchan*, 1988]. The NO_x emission was varied between 2.0×10^9 and 1.3×10^{11} molecules/cm^2/s, while VOCs, CO, CH_4, and photolysis frequencies were constrained by measurements and by using the Tropospheric Ultraviolet and Visible (TUV) radiation model [*Madronich and Flocke*, 1999]. In order to allow for spin-up time the box model was run for five consecutive diurnal cycles. Diurnal profiles typically did not change after the second day and the calculated output on day 5 was used for further analysis. Table 3 summarizes various model runs for clear skies and 30% cloud cover at noon on day 5 of the model output. The 30% cloud cover was approximated by linearly scaling TUV photolysis frequencies between the clear sky and 100% cloud cover case. The ozone mixing ratios calculated by the model scenarios were compared to measured ozone mixing ratios (10–20 ppbv in the PBL). Emission scenarios summarized in lines 2 and 3 in Table 3 simulated the measured ozone mixing ratios best and were subsequently used to constrain the box model along the altitude profile using the second box model setup. For these runs the MM model was initialized as a non-diluting zero-dimensional box constrained by NO_x (two scenarios), VOCs, CO, CH_4, NO_x, J-values and O_3. Photolysis rates were based on separate altitude dependent model runs using the Tropospheric Ultraviolet and Visible (TUV) radiation model for clear sky, 30%, and 100% cloud cover conditions. The TUV model was initialized according to "green ocean" cloud conditions [*Andreae et al.*, 2004; *Rosenfeld and Lensky*, 1998] resulting in a cloud optical depth (τ_{cl}) of ~40. The cloud to clear sky ratio of calculated photolysis frequencies (i.e., $j(O1D)$, $j(NO_2)$, $j(CH_2O)$, $j(H_2O_2)$) changed from about 0.4 below the cloud to 2.4 above the cloud and was within 15% for different species. It is noted that TUV is a one-dimensional radiative transfer model and could underestimate photolysis frequencies by neglecting edge effects between clouds in a broken cloud deck, which could only be determined using a true three-dimensional radiation model or measurements. The box model was then allowed to run to steady state. While all primary biogenic VOCs (isoprene and monoterpenes) as well as some important oxygenated VOCs (methanol, acetaldehyde, and acetone), CO, CH_4, NO_x, and *J*-values were held fixed, MVK and MAC were not constrained by our measurements and allowed to be calculated by the box model. The resulting (MVK + MAC)/isoprene ratios from this calculation are plotted together with the measured ratios (left panel). The measured ratios (implicitly MVK + MAC) are reproduced within the uncertainty of the model assumptions. The only exception appears to coincide with the top of the cloud deck (lower FT), where the measured ratio decreases significantly. This decrease could be caused by cloud venting, which transports photochemically less aged air masses from the PBL into the lower FT through active clouds. It is noted that vertical transport time in these model runs is not taken into account as the model was run to steady state. Figure 7 can be used to investigate the impact of vertical transport time on the photochemical age. The mean measured (MVK + MAC)/isoprene ratios increase from 0.39 to 0.61 at the top of the PBL (1200 m). This change puts constraints on a vertically increasing photochemical age in the PBL. We can use the convective velocity scale (equation (3)), which was calculated to be 1.9 m/s during profile measurements, as a measure for vertical mixing in the PBL. Further, a sequential reaction model (assuming that the reaction with OH is considerably more important than with O_3 during daytime, e.g., *Apel et al.* [2002]) can be simplified to the following analytical expression for the ratio between (MVK + MAC)/isoprene:

$$\frac{\mathrm{MVK + MAC}}{\mathrm{Isoprene}} = 0.55 \cdot \frac{k_{\mathrm{iso}}}{k_{\mathrm{iso}} - k_{\mathrm{carbonyl}}} \cdot \left[1 - \exp\left((k_{\mathrm{iso}} - k_{\mathrm{carbonyl}}) \cdot \mathrm{OH} \cdot \mathrm{t}\right)\right] \quad (5a)$$

$$t := \frac{z_i}{w^*} \quad (5b)$$

where 0.55 is total yield of MVK + MAC from the OH + isoprene reaction, k_{iso} is the reaction rate constant of isoprene + OH, $k_{carbonyl}$ is the average reaction rate constant of (MVK and MAC) + OH, z_i is the PBL depth, and w^* is the convective velocity scale. The resulting average OH density needed to explain this ratio at different heights in the PBL would be $4.3 \pm 2.4 \times 10^6$ molecules/cm^3. Similar analysis by *Kuhn et al.* [2007] showed OH concentrations on the order of $3-8 \times 10^6$ molecules/cm^3 for Manaus during LBA-CLAIRE-2001. For comparison the right panel in Figure 7 shows the resulting altitude profiles for modeled OH at 30% cloud cover and low NO_x conditions (180 pptv NO_x; Table 3, emission scenario 2) and 100% cloud cover and high NO_x conditions (320 pptv NO_x; Table 3, emission scenario 3). We also plot cases for low NO_x and high cloud cover and high NO_x and low cloud cover conditions. For all scenarios, the OH concentration increases toward the top of the PBL and CL due to enhanced photolysis rates and increasing ozone mixing ratios at higher altitudes ($\sim$7 ppbv at the bottom of the PBL and 19 ppbv above the CL). Direct experimental data reported by *Mauldin et al.* [1997] indicate significant OH changes above and in cloud decks due to cloud edge effects on photolysis rates which has a significant impact on OH production rates. We can compare these modeled OH profiles with PBL values estimated from the mixed box technique (section 3.1.4). Based on the NCAR MM, the OH values modeled for the PBL layer for four cases ((1) 180 pptv NO_x, 100% cloud cover, (2) 320 pptv NO_x, 100% cloud cover, (3) 180 pptv NO_x, 30% cloud cover, and (4) 320 pptv NO_x, 30% cloud cover) are $1.4 \pm 0.2 \times 10^5$, $2.9 \pm 0.4 \times 10^5$, $2.2 \pm 0.3 \times 10^5$, and $5.0 \pm 0.8 \times 10^5$ molecules/cm^3, respectively. These calculated OH concentrations are 3–10 times smaller than $1.3 \pm 0.5 \times 10^6$ molecules/cm^3 inferred from the MB method (section 3.1.3). For comparison, OH concentrations obtained from a simplified sequential reaction model output (equation (5)) are $4.3 \pm 2.4 \times 10^6$ molecules/cm^3. Based on upper and lower limits of calculated OH profiles (Figure 7), the difference between OH modeled using the NCAR MM and the MB method only partially arises from modeling assumptions (that is, modeled photolysis rates below the cloud deck, uncertainties associated with NO_x emission scenarios, and concentrations). Our measurements suggest that OH concentrations in the PBL calculated from the MB technique as well as a sequential reaction model constrained by measured vertical transport times are systematically higher than those modeled with a detailed zero-dimensional chemical box model. A similar conclusion has been drawn by *Kuhn et al.* [2007] during the end of the wet season. With respect to regional and global chemistry and transport models, increased OH production in broken clouds could offset this bias for the entire lower atmosphere. For comparison, the range of average OH densities (Figure 7) throughout the whole lower atmosphere (PBL plus CL) modeled according to the NCAR MM ($0.7-1.5 \pm 10^6$ molecules/cm^3) falls close to values calculated according to equation (4). However, this would not reconcile the discrepancy for box model simulations in the PBL. Alkene plus ozone reactions [*Atkinson*, 1997] are known to produce OH. Large biogenic sources of OH have recently been hypothesized above northern latitude forests [*di Carlo et al.*, 2004, *Kurpius and Goldstein*, 2003]. Assuming an OH yield of 1, the current monoterpene distribution (Figure 3) could lead to an additional OH density of 8×10^4 molecules/cm^3, which was not accounted for using the NCAR MM model. This would not be enough to explain the difference between box model simulations and mixed layer budget analysis. However, if we assume that reactive sesquiterpenes, such as β-caryophyllene, were present at mixing ratios of 10% of total monoterpene mixing ratios (or $\sim$1% of isoprene mixing ratios), it would be enough to produce an additional OH density of $\sim 4.5 \times 10^5$ molecules/cm^3. Direct measurements of these reactive terpenes have proven to be extremely difficult and, to this point, no reliable data sets are available. Direct evidence [*Karl et al.*, 2005; *Helmig et al.*, 2007; *Howard et al.*, 1988; *Langenheim et al.*, 1978] shows that a variety of Amazonian and North American tree species produce sesquiterpenes. Our recent measurements (unpublished results) show an ecosystem-scale sesquiterpene emission potential of 10% relative to monoterpenes in a northern latitude mixed forest and a subalpine pine forest. Future measurements of reactive VOCs along with photolysis rates, OH and HO_2, isoprene, and MVK + MAC will be crucial in determining sources and sinks of OH in the tropical atmosphere.

[32] An additional effect which could add to the modeling uncertainty in the lower atmosphere stems from the fact that the PBL and CL are strongly coupled layers influencing the distribution of radicals and biogenic VOCs. One of the consequences is that this could lead to segregation effects of oxidants and reactive VOCs such as isoprene.

3.4. Segregation Effects of Isoprene Chemistry

[33] The intensity of segregation (I_s) (defined as a relative reduction of the reaction rate constant due to incomplete mixing) of a VOC with respect to the OH radical is generally described as the covariance between the VOC and OH divided by the mean of each quantity [*Verver et al.*, 2000]:

$$I_s = \frac{\overline{VOC' \cdot OH'}}{\overline{VOC} \cdot \overline{OH}} \tag{6a}$$

An effective reaction rate constant for the atmosphere is then defined as:

$$k_{eff} = k \cdot (1 + I_s) \tag{6b}$$

with k as the reaction rate of OH and VOC and I_s as the intensity of segregation (range: -1 to $+1$). The intensity of segregation between two reactive species is therefore a measure of the effect of incomplete mixing between them. Previous studies have investigated species that are entrained from the free troposphere and may be segregated from species that are emitted from the surface. For example, if I_s was -0.5, the effective reaction rate in the atmosphere would be 50% lower than the laboratory rate constant measured under well-mixed conditions. *Krol et al.* [2000] state that a high spatial variation of VOCs emitted at the surface may generate an anti-correlated variability with OH. Here we investigate the effect of spatial variations of VOCs in and between clouds.

[34] The effect of segregation was estimated using the fast measurement capabilities of the PTR-MS instrument and water vapor as a proxy for OH. The averaging interval was

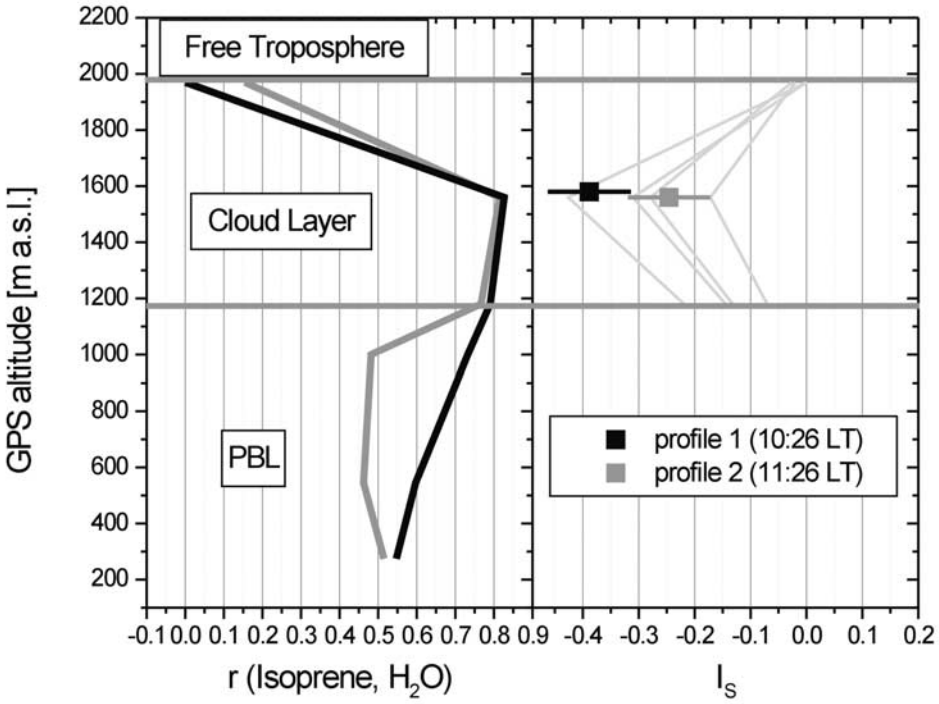

Figure 8. Left panel: Correlation coefficient between isoprene and H_2O plotted as a function of altitude for two profiles. Right panel: Lower and upper limits of the intensity of segregation (I_s) for isoprene and OH calculated for two profiles. Square symbols represent mean values of several independent parameterizations used to calculate I_s. Thin gray lines represent individual I_s calculations.

each flight level (i.e., 5 min) using 10 Hz measurements, corrected for instrumental noise. Within the cloud layer, we observed strong positive correlation between isoprene (M/Z 69) and $(H_3O)H_2O^+$ (M/Z 37) (Figure 8, left panel). Significant positive correlation in the CL indicates that isoprene-rich air is enhanced inside of clouds and depleted in air in between clouds, which has been entrained from the free troposphere. Our observations therefore indicate a spatially segregated isoprene distribution in the CL. This information is used in combination with observations of OH inside and outside of clouds [*Mauldin et al.*, 1997] and modeled OH distributions obtained from Figure 7.

[35] We define the smallest H_2O concentrations observed in the CL (0.9 mg/cm^3) as cloud-free and the maximum H_2O concentration (1.5 mg/cm^3) as air inside of clouds, which was visually confirmed on board of the aircraft. Next, we assign OH densities to these two CL regimes (cloud and cloud-free) and calculate a segregation density according to:

$$I_s = \frac{\overline{\mathrm{VOC}' \cdot (\mathrm{scaling} \cdot \mathrm{H_2O})'}}{\overline{\mathrm{VOC}} \cdot \overline{(\mathrm{scaling} \cdot \mathrm{H_2O})}} \qquad (6c)$$

[36] The scaling factor in (6c) is based on (1) measured OH profiles in clouds [*Mauldin et al.*, 1997] (4.8-fold decrease of OH inside cloud), (2) upper, (3) lower limit gas-phase model calculations of OH summarized in Figure 7, and (4) model calculations presented by *Barth et al.* [2003]. In all cases, the scaling is linearly interpolated according to the measured H_2O concentration between the two extremes (cloud-free and cloud). For modeled OH (cases 2 and 3), we assign the OH density inside a cloud parcel according to the OH density calculated at the top of the PBL (1200 m asl); the cloud-free OH density is taken according to values calculated just above the cloud deck (2000 m asl). We neglect the impact of aqueous-phase chemistry on the I_s calculation. In a sensitivity study, Barth et al. reported a 40% change of OH between cloud and cloud-free conditions using a photochemical box model with limited hydrocarbon chemistry, but detailed aqueous-phase chemistry. Due to the inherent modeling uncertainties, we give the scenarios based on measured OH concentrations the most weight. It is noted that the I_s calculation is only sensitive to the relative difference of OH between cloud and cloud-free conditions. Figure 8 (right panel) plots segregation effects for two profiles flown above Z14 on 6 September using the approaches described above. We assume well-mixed conditions in the PBL layer. The presented segregation approach is therefore not applicable for the PBL. Black colors indicate values calculated for the first profile and gray colors depict the segregation observed for the second profile ($\sim$1 h later). Shown in Figure 8 are the mean and standard deviation for all four scenarios as well as individual I_s profiles depicted by thin gray lines. Values obtained based on *Mauldin et al.* [1997] give typically the highest intensity of segregation (-44 and -29% for profiles 1 and 2). These are close to the parameterization based on the upper limit of OH model scenarios calculated using the NCAR MM (section 3.3) (-47 and -33% for profiles 1 and 2). Based on the study of *Barth et al.* [2003], we calculate an

I_s of −34 and −20% for profiles 1 and 2, which are close to the parameterization using the lower limit of OH calculated by the NCAR MM model scenarios (−31 and −17%). The second profile showed a slightly lower correlation between water and isoprene, resulting in a decrease of the segregation effect most likely due to better-mixed conditions encountered during the second profile. Future measurements of OH in conjunction with fast VOC measurements could be used to investigate segregation effects throughout the whole atmosphere in more detail. Here we show that these effects can be important in broken cloud decks.

4. Conclusion

[37] Deployment of new in situ instrumentation (PTR-MS and FTIR) together with traditional canister and cartridge sampling proved to be a powerful combination for investigating the fate of reactive biogenic VOCs emitted in the Amazon basin. High VOC sampling rates allowed calculating fluxes of isoprene and monoterpenes using the Mixed Layer Gradient and Mixed Layer Variance techniques. Comparison with ground-based eddy covariance measurements showed reasonable agreement. Average noontime isoprene and monoterpenes fluxes were 7.8 ± 2.3 and 1.2 ± 0.5 mg/m^2/h, respectively. Isoprene and monoterpene fluxes corrected to standard conditions (30°C, 1000 PAR) on the ground were 5.9 ± 0.1 and 1.2 ± 0.1 mg/m^2/h, respectively. The monoterpene composition inferred from GC-MS measurements was dominated by α-pinene (38%), β-pinene (20%), limonene (18%), and sabinene (11%). Smaller amounts of camphene (4%), myrcene (2%), and 3-carene (7%) were also detected in the samples. Isoprene and monoterpenes accounted for ~75% of the total reactivity with respect to the OH radical.

[38] We observed altered isoprene emissions above areas strongly influenced by agricultural land-use change (i.e., soybean plantations). In general, a bottom-up emission model (MEGAN) reproduced isoprene emissions above different land-cover types reasonably well within the model and measurement uncertainty. This contrasts various global modeling and HCHO retrieval studies that suggest the opposite.

[39] Our observations show evidence that the formation of a broken cloud deck (*cumulus humilis*) can significantly influence the redistribution of reactive VOCs such as isoprene by (1) entraining free tropospheric air, (2) venting PBL air through active clouds, (3) enhancing the oxidative capacity of the atmosphere, and (4) segregating OH and VOCs emitted at the surface. VOC entrainment rates between 10:00 and 11:30 local time, for example, were on the order of 30% of their surface emissions. The calculated effect of segregation obtained from this study could reduce the effective reactivity of isoprene up to 39 ± 7% in the cloud layer. The effective rate constant of isoprene and OH can therefore vary significantly in different parts of the lower atmosphere. Modeled OH concentrations using a detailed photochemical box model were lower in the PBL than those calculated using the MB approach and a sequential reaction model constrained by vertical transport timescales. The presence of ozone-reactive terpenes could explain this difference if their mixing ratios added up to at least 1% of isoprene mixing ratios.

[40] Additional effects, in particular changes of OH radical concentrations in the CL, caused by the presence of clouds can lead to significant uncertainties of modeled isoprene concentrations observed by many large-scale regional and global 3D-CT models under weak synoptic forcing (i.e., in the tropics). Since these models do not resolve processes on length and timescales typical for the PBL, this might contribute to the uncertain model predictions of short-lived compounds in the tropics. Future studies addressing these uncertainties in more detail are therefore needed in order to lead to reliable parameterizations of emissions and characteristic PBL processes of reactive VOCs in the tropical atmosphere.

[41] **Acknowledgments.** The authors thank our pilots Pedro Celso and Alexandro Pele as well as Joao Carvalho, Peter Harley, Antonio Ocimar Manzi, Julio Tota, and Gioberto Nishioka for excellent logistical support and vital collaboration in Brazil. We also thank Sasha Madronich for providing a version of the TUV code and Christine Wiedinmyer and Craig Stroud for an updated version of the NCAR MM code. Yokelson was supported by NSF grant ATM0228003 and the Rocky Mountain Research Station, Forest Service, U.S. Department of Agriculture (INT-97082-RJVA and RMRS 99508 RJVA). The National Center for Atmospheric Research is sponsored by the National Science Foundation.

References

Albrecht, B. A., R. S. Penc, and W. H. Schubert (1985), An observational study of cloud-topped mixed layers, *J. Atmos. Sci.*, *42*(8), 800–822.

Andreae, M. O., et al. (2002), Biogeochemical cycling of carbon, water, energy, trace gases, and aerosols in Amazonia: The LBA-EUSTACH experiments, *J. Geophys. Res.*, *107*(D20), 8066, doi:10.1029/2001JD000524.

Andreae, M. O., et al. (2004), Smoking rain clouds over the Amazon, *Science*, *303*(5662), 1337–1342.

Angevine, W. M. (2005), An integrated turbulence scheme for boundary layers with shallow cumulus applied to pollutant transport, *J. Appl. Meteorol.*, *44*, 1436–1452.

Apel, E. C., et al. (2002), Measurement and interpretation of isoprene fluxes and isoprene, methacrolein, and methyl vinyl ketone mixing ratios at the PROPHET site during the 1998 Intensive, *J. Geophys. Res.*, *107*(D3), 4034, doi:10.1029/2000JD000225.

Atkinson, R. (1997), Gas-phase tropospheric chemistry of volatile organic compounds: 1. Alkanes and alkenes, *J. Phys. Chem. Ref. Data*, *26*, 215–290.

Barth, M. C., et al. (2003), Summary of the cloud chemistry modeling intercomparison: Photochemical box model simulation, *J. Geophys. Res.*, *108*(D7), 4214, doi:10.1029/2002JD002673.

Baumann, K., et al. (2000), Ozone production and transport near Nashville, Tennessee: Results from the 1994 study at New Hendersonville, *J. Geophys. Res.*, *105*(D7), 9137–9153.

Bey, I., et al. (2001), Global modeling of tropospheric chemistry with assimilated meteorology: Model description and evaluation, *J. Geophys. Res.*, *106*(D19), 23,073–23,095.

Ching, J. K. S., and A. J. Alkezweeny (1986), Trace study of vertical exchange by cumulus clouds, *J. Clim. Appl. Meteorol.*, *25*, 1702–1711.

Crutzen, P. J., et al. (2000), High spatial and temporal resolution measurements of primary organics and their oxidation products over the tropical forests of Surinam, *Atmos. Environ.*, *34*(8), 1161–1165.

de Gouw, J. A., et al. (2003), Validation of proton transfer reaction-mass spectrometry (PTR-MS) measurements of gas-phase organic compounds in the atmosphere during the New England Air Quality Study (NEAQS) in 2002, *J. Geophys. Res.*, *108*(D21), 4682, doi:10.1029/2003JD003863.

di Carlo, P., et al. (2004), Missing OH reactivity in a forest: Evidence for unknown reactive biogenic VOCs, *Science*, *304*, 722–725.

Donoso, L., et al. (1996), Natural and anthropogenic C2 to C6 hydrocarbons in the central-eastern Venezuelan atmosphere during the rainy season, *J. Atmos. Chem.*, *25*, 201–214.

Ehhalt, D., and M. Prather (2001), *Atmospheric Chemistry and Greenhouse Gases. Climate Change 2001; Working Group 1: The Scientific Basis*, Cambridge Univ. Press, New York.

Fall, R., T. Karl, A. Jordon, and W. Lindinger (2001), Biogenic C5VOCs: Release from leaves after freeze-thaw wounding and occurrence in air at a high mountain observatory, *Atmos. Environ.*, *35*(22), 3905–3916.

Faloona, I., et al. (2005), Observations of entrainment in eastern Pacific marine stratocumulus using three conserved scalars, *J. Atmos. Sci.*, *62*(9), 3268–3285.

Fisch, G., et al. (2004), The convective boundary layer over pasture and forest in Amazonia, *Theor. Appl. Climatol.*, *78*(1–3), 47–59.

Fuentes, J. D., et al. (2000), Biogenic hydrocarbons in the atmospheric boundary layer: A review, *Bulletin of the American Meteorological Society, Impact of Global Climatic Changes on Photosynthesis and Plant Productivity: Proceedings of the Indo-US Workshop held on January 8–12, 1991 at New Delhi, India*, *81*(7), 1537–1576.

Ganzeveld, L. N., J. Lelieveld, F. J. Dentener, M. C. Krol, and G. J. Roelofs (2002), Atmosphere-biosphere trace gas exchanges simulated with a single-column model, *J. Geophys. Res.*, *107*(D16), 4320, doi:10.1029/2001JD000684.

Greenberg, J. P., and P. R. Zimmerman (1984), Nonmethane hydrocarbons in remote tropical, continental, and marine atmospheres, *J. Geophys. Res.*, *89*(ND3), 4767–4778.

Greenberg, J., B. Lee, D. Helmig, and P. Zimmerman (1994), Fully automated gas chromatograph-flame ionization detector system for the in situ determination of atmospheric non-methane hydrocarbons at low parts per trillion concentration, *J. Chromatogr.*, *676*, 389–398.

Greenberg, J. P., et al. (1999a), Tethered balloon measurements of biogenic VOCs in the atmospheric boundary layer, *Atmos. Environ.*, *33*(6), 855–867.

Greenberg, J. P., et al. (1999b), Biogenic volatile organic compound emissions in central Africa during the Experiment for the Regional Sources and Sinks of Oxidants (EXPRESSO) biomass burning season, *J. Geophys. Res.*, *104*(Part D23), 30,659–30,672.

Greenberg, J. P., et al. (2004), Biogenic VOC emissions from forested Amazonian landscapes, *Global Change Biol.*, *10*(5), 651–662.

Gregory, G., et al. (1986), Air chemistry over the tropical forest of Guyana, *J. Geophys. Res.*, *91*, 8603–8612.

Griffin, R. J., D. R. Cocker, R. C. Flagan, and J. H. Seinfeld (1999), Organic aerosol formation from the oxidation of biogenic hydrocarbons, *J. Geophys. Res.*, *104*, 3555–3567.

Guenther, A., C. N. Hewitt, D. Erickson, and R. Fall (1995), A global model of natural volatile organic compound emissions, *J. Geophys. Res.*, *100*(D/5), 8873–8892.

Guenther, A., et al. (2006), Estimates of global terrestrial isoprene emissions using MEGAN (Model of Emissions of Gases and Aerosols from Nature), *Atmos. Chem. Phys.*, *6*, 3181–3210.

Hansel, A., A. Jordan, C. Warneke, R. Holzinger, and W. Lindinger (1998), Improved detection limit of the proton-transfer reaction mass spectrometer: On-line monitoring of volatile organic compounds at mixing ratios of a few PPTV, *Rapid Commun. Mass Spectrom.*, *12*(13), 871–875.

Harley, P., et al. (2004), Variation in potential for isoprene emissions among neotropical forest sites, *Global Change Biol.*, *10*(5), 630–650.

Hauglustaine, D. A., et al. (1996), Observed and model-calculated photostationary state at Mauna Loa Observatory during MLOPEX 2, *J. Geophys. Res.*, *101*, 14,681–14,696.

Helmig, D., et al. (1998), Vertical profiling and determination of landscape fluxes of biogenic nonmethane hydrocarbons within the planetary boundary layer in the Peruvian Amazon, *J. Geophys. Res.*, *103*(D19), 25,519–25,532.

Helmig, D., J. Ortega, T. Duhl, D. Tanner, A. Guenther, P. Harley, C. Wiedinmyer, J. Milford, and T. Sakulyanontvittaya (2007), Sesquiterpene emissions from pine trees: Identifications, emission rates and flux estimates for the contiguous United States, *Environ. Sci. Technol.*, *41*, 1545–1553.

Holzinger, R., et al. (2002), Diurnal cycles and seasonal variation of isoprene and its oxidation products in the tropical savanna atmosphere, *Global Biogeochem. Cycles*, *16*(4), 1074, doi:10.1029/2001GB001421.

Howard, J. J., J. Coxing, and D. Wiemer (1988), Toxicity of terpenoid detergents to the leaf-cutting ant *Atta cephalotes* and its mutualistic funus, *J. Chem. Ecol.*, *14*, 59–69.

Jacob, D. J., and S. C. Wofsy (1988), Photochemistry of biogenic emissions over the Amazon forest, *J. Geophys. Res.*, *93*, 1477–1486.

Kaplan, W. A., S. C. Wofsy, M. Keller, and J. M. Dacosta (1988), Emission of NO and deposition of O-3 in a tropical forest system, *J. Geophys. Res.*, *93*(D2), 1389–1395.

Karl, T., et al. (2001), Eddy covariance measurements of oxygenated volatile organic compound fluxes from crop harvesting using a redesigned proton-transfer-reaction mass spectrometer, *J. Geophys. Res.*, *106*(Part 20), 24,157–24,168 (Paper 2000JD000112).

Karl, T. G., et al. (2002), Virtual disjunct eddy covariance measurements of organic compound fluxes from a subalpine forest using proton transfer reaction mass spectrometry, *Atmos. Chem. Phys.*, *2*, 279–291.

Karl, T., et al. (2004), Exchange processes of volatile organic compounds above a tropical rain forest: Implications for modeling tropospheric chemistry above dense vegetation, *J. Geophys. Res.*, *109*(D18), D18306, doi:10.1029/2004JD004738.

Karl, T., P. Harley, A. Guenther, R. Rasmussen, B. Baker, K. Jardine, and E. Nemitz (2005), The bi-directional exchange of oxygenated VOCs between a loblolly pine (*Pinus taeda*) plantation and the atmosphere, *Atmos. Chem. Phys.*, *5*, 3015–3031.

Kesselmeier, J., et al. (2000), Atmospheric volatile organic compounds (VOC) at a remote tropical forest site in central Amazonia, *Atmos. Environ.*, *34*(24), 4063–4072.

Kesselmeier, J., et al. (2002), Concentrations and species composition of atmospheric volatile organic compounds (VOCs) as observed during the wet and dry season in Rondonia (Amazonia), *J. Geophys. Res.*, *107*(D20), 8053, doi:10.1029/2000JD000267.

Krol, M. C., M. J. Molemaker, and J. V. G. de Arellano (2000), Effects of turbulence and heterogeneous emissions on photochemically active species in the convective boundary layer, *J. Geophys. Res.*, *105*(D5), 6871–6884.

Kuhlmann, R. V., M. Lawrence, and P. J. Crutzen (2003), Sensitivities in global scale modeling of isoprene, *Atmos. Chem. Phys.*, *3*, 3095–3134.

Kuhn, U., et al. (2002), Isoprene and monoterpene emissions of Amazonian tree species during the wet season: Direct and indirect investigations on controlling environmental functions, *J. Geophys. Res.*, *107*(D20), 8071, doi:10.1029/2001JD000978.

Kuhn, U., et al. (2004), Seasonal differences in isoprene and light-dependent monoterpene emission by Amazonian tree species, *Global Change Biol.*, *10*(5), 663–682.

Kuhn, U., et al. (2007), Isoprene and monoterpene fluxes from Central Amazonian rainforest inferred from tower-based and airborne measurements, and implications on the atmospheric chemistry and the local carbon budget, *Atmos. Chem. Phys. Disc.*, *7*, 641–708.

Kurpius, M. R., and A. H. Goldstein (2003), Gas-phase chemistry dominates O_3 loss to a forest, implying a source of aerosols and hydroxyl radicals to the atmosphere, *Geophys. Res. Lett.*, *30*(7), 1371, doi:10.1029/2002GL016785.

Langenheim, J., C. Foster, D. Lincoln, and W. Stubblebine (1978), Implications of variation in resin composition among organs, tissues and populations in the tropical legume *Hymenara*, *Biochem. Syst. Ecol.*, *8*, 385–396.

Lenschow, D. H., J. Mann, and L. Kristensen (1994), How long is long enough when measuring fluxes and other turbulence statistics, *J. Atmos. Oceanic Technol.*, *11*(3), 661–673.

Lenschow, D. H., et al. (1999), Use of a mixed-layer model to estimate dimethylsulfide flux and application to other trace gas fluxes, *J. Geophys. Res.*, *104*(D13), 16,275–16,295.

Lindinger, W., A. Jordan, and A. Hansel (1998), Proton-transfer-reaction mass spectroscopy (PTR-MS): On-line monitoring of volatile organic compounds at pptv levels, *Chem. Soc. Rev.*, *27*, 347–534.

Lindinger, W., R. Fall, and T. Karl (2001), Environmental, food and medical applications of proton-transfer-reaction mass spectrometry (PTR-MS), in: *Advances in Gas-Phase Ion Chemistry*, edited by N. G. Adams, pp. 1–35, Elsevier, New York.

Madronich, S., and J. Calvert (1990), Permutation reactions of organic peroxy radicals in the troposphere, *J. Geophys. Res.*, *95*, 5697–5715.

Madronich, S., and S. Flocke (1999), The role of solar radiation in atmospheric chemistry, in *Handbook of Environmental Chemistry*, edited by P. Boule, p. 1–26, Springer, New York.

Mauldin, R. L., et al. (1997), New insights on OH: Measurements around and in clouds, *Geophys. Res. Lett.*, *24*(23), 3033–3036.

Olivier, J. G. J., and J. J. M. Berdowski (2001), Global emissions sources and sinks, in: *The Climate System*, edited by J. G. J. Olivier, J. J. M. Berdowski, R. Guicherit, and B. J. Heij, pp. 33–78, A. A. Balkema, Brookfield, Vt.

Palmer, P. I., et al. (2003), Mapping isoprene emissions over North America using formaldehyde column observations from space, *J. Geophys. Res.*, *108*(D6), 4180, doi:10.1029/2002JD002153.

Patton, E. G., K. J. Davis, M. C. Barth, and P. P. Sullivan (2001), Decaying scalars emitted by a forest canopy: A numerical study, *Boundary Layer Meteorol.*, *100*(1), 91–129.

Patton, E. G., P. P. Sullivan, and C. H. Moeng (2005), The influence of idealized heterogeneity on wet and dry planetary boundary layers coupled to the land surface, *J. Atmos. Sci.*, *62*(7), 2078–2097.

Petron, G., P. Harley, J. Greenberg, and A. Guenther (2001), Seasonal temperature variations influence isoprene emission, *Geophys. Res. Lett.*, *28*(9), 1707–1710.

Rasmussen, R. A., and M. A. K. Khalil (1988), Isoprene over the Amazon Basin, *J. Geophys. Res.*, *93*(D2), 1417–1421.

Rinne, H. J. I., A. B. Guenther, C. Warneke, J. A. de Gouw, and S. L. Luxembourg (2001), Disjunct eddy covariance technique for trace gas flux measurements, *Geophys. Res. Lett.*, *28*(16), 3139–3142.

Rinne, H. J. I., A. B. Guenther, J. P. Greenberg, and P. C. Harley (2002), Isoprene and monoterpene fluxes measured above Amazonian rainforest and their dependence on light and temperature, *Atmos. Environ.*, *36*(14), 2421–2426.

Rosenfeld, D., and I. M. Lensky (1998), Satellite-based insights into precipitation formation processes in continental and maritime convective clouds, *Bull. Am. Meteorol. Soc.*, *79*(11), 2457–2476.

Sanhueza, E., et al. (1996), Field measurement evidence for an atmospheric chemical source of formic and acetic acids in the tropics, *Geophys. Res. Lett.*, *23*(9), 1045–1048.

Shim, C., et al. (2005), Constraining global isoprene emissions with Global Ozone Monitoring Experiment (GOME) formaldehyde column measurements, *J. Geophys. Res.*, *110*(D24), D24301, doi:10.1029/2004JD005629.

Spirig, C., A. Guenther, J. P. Greenberg, P. Calanca, and V. Tarvainen (2004), Tethered balloon measurements of biogenic volatile organic compounds at a boreal forest site, *Atmos. Chem. Phys.*, *4*, 215–229.

Spirig, C., et al. (2005), Eddy covariance flux measurements of biogenic VOCs during ECHO 2003 using proton transfer reaction mass spectrometry, *Atmos. Chem. Phys.*, *5*, 465–481.

Stull, R. (1988), *An Introduction to Boundary Layer Meteorology*, Springer, New York.

Torres, A. L., and H. Buchan (1988), Tropospheric nitric-oxide measurements over the Amazon Basin, *J. Geophys. Res.*, *93*(D2), 1396–1406.

Trainer, M., et al. (1987), Impact of natural hydrocarbons on hydroxyl and peroxy-radicals at a remote site, *J. Geophys. Res.*, *92*(D10), 11,879–11,894.

Verver, G. H. L., H. van Dop, and A. A. M. Holtslag (2000), Turbulent mixing and the chemical breakdown of isoprene in the atmospheric boundary layer, *J. Geophys. Res.*, *105*(D3), 3983–4002.

Vinuesa, J. F., and J. V. G. de Arellano (2005), Introducing effective reaction rates to account for the inefficient mixing of the convective boundary layer, *Atmos. Environ.*, *39*(3), 445–461.

Warneke, C., et al. (2001), Isoprene and its oxidation products methyl vinyl ketone, methacrolein, and isoprene related peroxides measured online over the tropical rain forest of Surinam in March 1998, *J. Atmos. Chem.*, *38*(2), 167–185.

Williams, J., et al. (2001), An atmospheric chemistry interpretation of mass scans obtained from a proton transfer mass spectrometer flown over the tropical rainforest of Surinam, *J. Atmos. Chem.*, *38*(2), 133–166.

Wyngaard, J., and R. Brost (1984), Top-down and bottom-up diffusion in the convective boundary layer, *J. Atmos. Sci.*, *41*, 102–112.

Yokelson, R. J., R. Susott, D. E. Ward, J. Reardon, and D. W. T. Griffith (1997), Emissions from smoldering combustion of biomass measured by open-path Fourier transform infrared spectroscopy, *J. Geophys. Res.*, *102*(D15), 18,865–18,877.

Yokelson, R. J., T. Karl, P. Artaxo, D. R. Blake, T. J. Christian, D. W. T. Griffith, A. Guenther, and W. M. Hao (2007), The tropical forest and fire emissions experiment: Overview and airborne fire emission factor measurements, *Atmos. Chem. Phys. Disc.*, *7*, 6903–6958. (Available at http://www.atmos-chem-phys-discuss.net/7/6903/2007/)

Zimmerman, P. R., J. P. Greenberg, and C. E. Westberg (1988), Measurements of atmospheric hydrocarbons and biogenic emission fluxes in the Amazon boundary-layer, *J. Geophys. Res.*, *93*(D2), 1407–1416.

P. Artaxo, University of Sao Paulo, Sao Paulo, Brazil.

D. R. Blake, Department of Chemistry, University of California, Irvine, CA, USA.

J. Greenberg, A. Guenther, and T. Karl, National Center for Atmospheric Research, Boulder, CO, USA. (tomkarl@ucar.edu)

M. Potosnak, Desert Research Institute, Reno, NV, USA.

R. J. Yokelson, Department of Chemistry, University of Montana, Missoula, MT, USA.